in the absence of phlorizin minus the glucose uptake in the presence of phlorizin.

Results

Insulin secretion in isolated islets

Insulin secretory responses of Kir6.2$^{-/-}$GIPR$^{-/-}$ mice were examined *in vitro* by batch incubation study. Total insulin content per single islet is decreased in Kir6.2$^{-/-}$ GIPR$^{-/-}$ mice compared with wild-type (Kir6.2$^{+/+}$ GIPR$^{+/+}$) mice (47.3± 3.5%, data not shown). In comparison with the basal level of insulin secretion at 2.8 mmol/l glucose from batch-incubated pancreatic islets, the insulin secretion in Kir6.2$^{-/-}$ GIPR$^{-/-}$ mice in response to 8.3 mmol/l glucose, 16.7 mmol/l glucose, 25.0 mmol/l glucose, 100 μmol/l tolbutamide in the presence of 16.7 mmol/l glucose or 100 nmol/l GIP in the presence of 8.3 mmol/l glucose is similar. In contrast, 100 nmol/l GLP-1 in the presence of 8.3 mmol/l glucose elicits an increased response (Fig. 1).

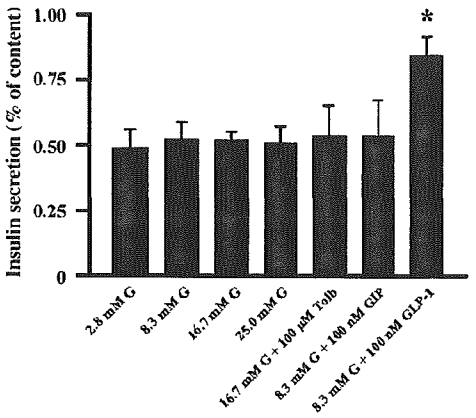

Figure 1 Insulin secretion from islets of Kir6.2$^{-/-}$GIPR$^{-/-}$ mice. Insulin secretion in batch-incubated pancreatic islets of Kir6.2$^{-/-}$ GIPR$^{-/-}$ mice in response to the indicated concentrations of glucose (G), 100 μmol/l tolbutamide (Tolb), 100 nmol/l GIP and 100 nmol/l GLP-1 are shown. Values are means±S.E.M., relative to the insulin content in averaged single islets of Kir6.2$^{-/-}$ GIPR$^{-/-}$ mice ($n = 40$). *$P < 0.05$ compared with 2.8 mmol/l glucose.

Immunohistochemistry of pancreatic islets

Immunohistochemical examination shows that the number of insulin-positive β-cells in islets of Kir6.2$^{-/-}$ GIPR$^{-/-}$ is increased, and that the area containing insulin-positive cells in the islets of Kir6.2$^{-/-}$GIPR$^{-/-}$ mice is increased by 32.6% compared with Kir6.2$^{-/-}$ GIPR$^{+/+}$ mice. Glucagon-positive α-cells, which are present primarily in the periphery in islets of Kir6.2$^{+/+}$ GIPR$^{+/+}$ mice, also appear in the central region in islets of Kir6.2$^{-/-}$GIPR$^{-/-}$ mice, as in Kir6.2$^{-/-}$ GIPR$^{+/+}$ mice (Fig. 2).

Glucose tolerance and insulin secretion in vivo

Fasting glucose levels are similar in Kir6.2$^{-/-}$ GIPR$^{-/-}$, Kir6.2$^{-/-}$GIPR$^{+/+}$, and Kir6.2$^{+/+}$GIPR$^{+/+}$ mice. However, after oral glucose loading, blood glucose

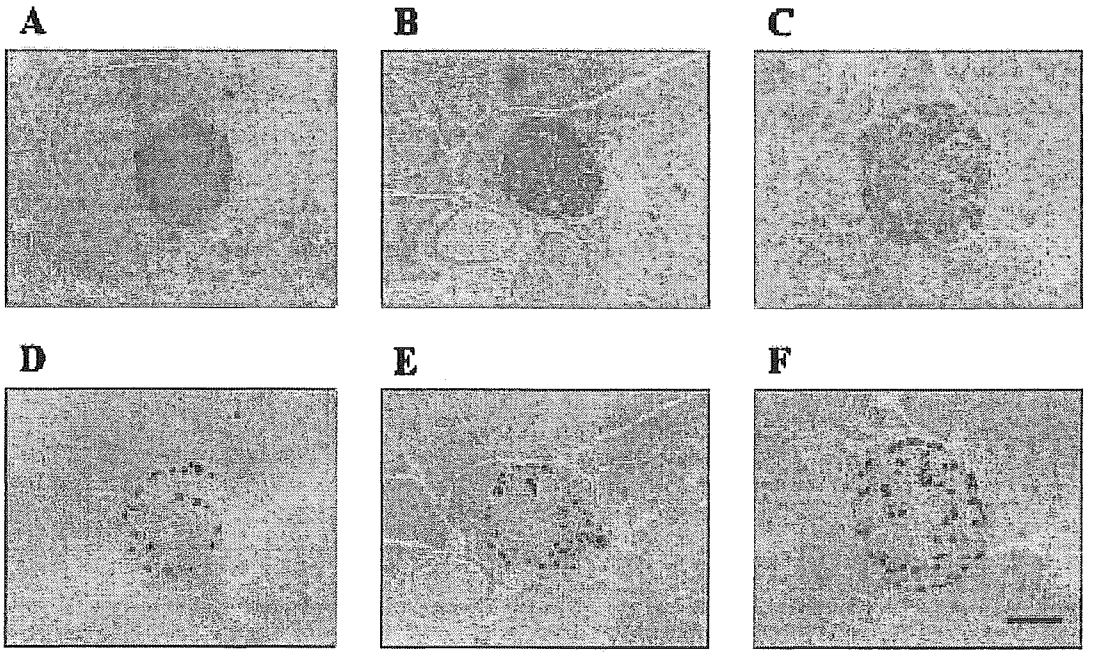

Figure 2 Immunohistochemical analyses of pancreatic islets. Immunohistochemical analyses of pancreatic islets of Kir6.2$^{+/+}$GIPR$^{+/+}$ mice (A, D), Kir6.2$^{-/-}$GIPR$^{+/+}$ mice (B, E), and Kir6.2$^{-/-}$GIPR$^{-/-}$ mice (C, F) are shown. Pancreatic β-cells and α-cells were stained using rabbit anti-insulin antibodies (A, B and C) or anti-glucagon antibodies (D, E and F). Bar = 100 μm.

levels of Kir6.2$^{-/-}$GIPR$^{-/-}$ mice become elevated compared with Kir6.2$^{-/-}$GIPR$^{+/+}$ mice, especially at 15 min (345±10 mg/dl vs 294±20 mg/dl, $P < 0.05$) and 30 min (453±20 mg/dl vs 381±26 mg/dl, $P < 0.05$) (Fig. 3A). The time of peak glucose response is at 30 min both in Kir6.2$^{-/-}$GIPR$^{-/-}$ mice and Kir6.2$^{-/-}$GIPR$^{+/+}$ mice. Plasma insulin levels were measured to determine the cause of the glucose intolerance in Kir6.2$^{-/-}$GIPR$^{-/-}$ mice. Fasting insulin levels in Kir6.2$^{-/-}$GIPR$^{-/-}$ mice and Kir6.2$^{-/-}$GIPR$^{+/+}$ mice are similar. The insulin response after oral glucose loading is almost completely lost in Kir6.2$^{-/-}$GIPR$^{-/-}$ mice, and the insulin levels at 15 min and 30 min in Kir6.2$^{-/-}$GIPR$^{-/-}$ mice are lower than in Kir6.2$^{-/-}$GIPR$^{+/+}$ mice (Fig. 3B), indicating that the glucose intolerance in Kir6.2$^{-/-}$GIPR$^{-/-}$ mice is due to insufficient insulin secretion.

Glucose uptake by the jejunum in vitro

We investigated glucose uptake by the jejunum *in vitro* using everted jejunal rings, and found no difference among Kir6.2$^{+/+}$GIPR$^{+/+}$, Kir6.2$^{-/-}$GIPR$^{+/+}$ and Kir6.2$^{-/-}$GIPR$^{-/-}$ mice (Fig. 4).

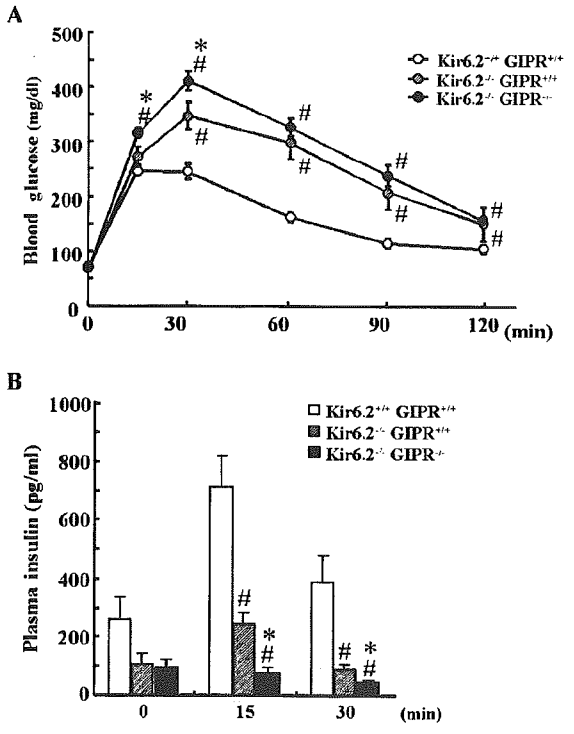

Figure 3 Glucose tolerance test. (A) Blood glucose levels after oral glucose loading are shown: Kir6.2$^{+/+}$GIPR$^{+/+}$ mice, open circles; Kir6.2$^{-/-}$GIPR$^{+/+}$ mice, hatched circles; Kir6.2$^{-/-}$GIPR$^{-/-}$ mice, solid circles ($n = 5$). (B) Plasma insulin levels after oral glucose tolerance test are shown: Kir6.2$^{+/+}$GIPR$^{+/+}$ mice, open bars; Kir6.2$^{-/-}$GIPR$^{+/+}$ mice, hatched bars; Kir6.2$^{-/-}$GIPR$^{-/-}$ mice, solid bars ($n = 5$). Values are means±S.E.M. #$P < 0.05$ vs Kir6.2$^{+/+}$GIPR$^{+/+}$ mice; *$P < 0.05$ vs Kir6.2$^{-/-}$GIPR$^{+/+}$ mice.

Insulin sensitivity in vivo

The glucose-lowering effect of insulin was assessed by an insulin tolerance test. Kir6.2$^{-/-}$GIPR$^{-/-}$ mice and Kir6.2$^{-/-}$GIPR$^{+/+}$ mice are similarly insulin sensitive, and more so than Kir6.2$^{+/+}$GIPR$^{+/+}$ mice (Fig. 5).

Discussion

GIP and GLP-1 are physiological incretins (7, 15) that stimulate insulin secretion from pancreatic β-cells upon ingestion of nutrients. GIP and GLP-1 bind to specific receptors, the GIPR and the GLP-1 receptor (GLP-1R), and increase the intracellular cAMP concentration, which produces insulin secretion. However, functional differences have become clear in recent studies of knockout mice (10, 16–18). GIPR$^{-/-}$ mice exhibit normal glucose tolerance after intraperitoneal glucose loading but impaired glucose tolerance after oral glucose loading, while GLP-1R-knockout (GLP-1$^{-/-}$) mice exhibit impaired glucose tolerance

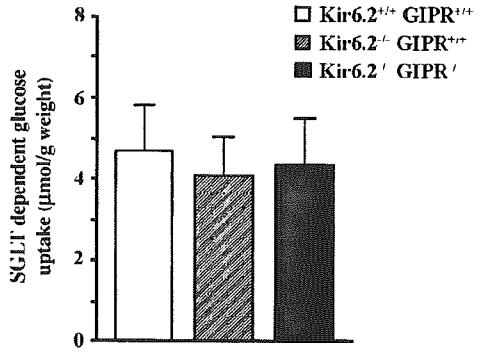

Figure 4 Glucose uptake in the jejunum. Glucose uptake in the jejunum in Kir6.2$^{+/+}$GIPR$^{+/+}$ mice, open bar; Kir6.2$^{-/-}$GIPR$^{+/+}$ mice, hatched bar; Kir6.2$^{-/-}$GIPR$^{-/-}$ mice, solid bar is shown ($n = 4$). Na^+/glucose cotransporter (SGLT)-dependent glucose uptake was determined as the glucose uptake in the absence of phlorizin minus the glucose uptake in the presence of 1 mmol/l phlorizin. Values are means±S.E.M.

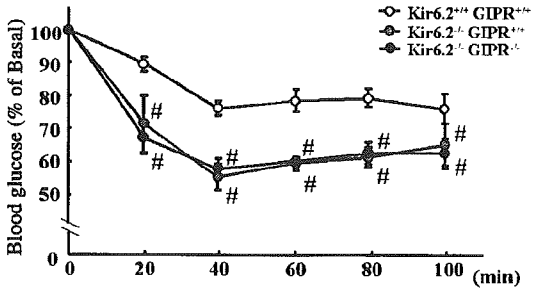

Figure 5 Insulin tolerance test. Changes in blood glucose levels upon insulin injection are shown: Kir6.2$^{+/+}$GIPR$^{+/+}$ mice, open circles; Kir6.2$^{-/-}$GIPR$^{+/+}$ mice, hatched circles; Kir6.2$^{-/-}$GIPR$^{-/-}$ mice, solid circles ($n = 5$). Values are means±S.E.M., relative to basal blood glucose levels. #$P < 0.05$ compared with Kir6.2$^{+/+}$GIPR$^{+/+}$ mice.

both orally and intraperitoneally. $GIPR^{-/-}$ mice also exhibit an increased number of pancreatic β-cells while $GLP\text{-}1R^{-/-}$ mice show a decreased number. In addition, GLP-1 causes a decreased gastric emptying rate by intravenous infusion in humans (19), and produces a marked reduction in food and water intake in rats through a central mechanism (20). Apparently, GIP contributes to glucose homeostasis by raising insulin secretion in response to an oral glucose load while GLP-1 contributes by pancreatic β-cell proliferation and other factors in addition to insulin secretion. In the present study using double-knockout mice, we establish that GIP is the insulinotropic factor in the insulin response to oral glucose loading in K_{ATP} channel-deficient mice. $Kir6.2^{-/-}GIPR^{-/-}$ mice show no increase in plasma insulin levels in response to an oral glucose load, demonstrating that the insulin secretory response in $Kir6.2^{-/-}GIPR^{+/+}$ mice to an oral glucose load is abolished in the absence of the GIP signal.

Immunohistochemical examination of pancreatic islets of $Kir6.2^{-/-}GIPR^{-/-}$ mice shows that the area containing insulin-positive β-cells is larger than in $Kir6.2^{-/-}GIPR^{+/+}$ islets at 18 weeks of age. It has been reported that the number of β-cells in $Kir6.2^{-/-}$ mice is similar to wild-type ($Kir6.2^{+/+}$) mice before 16 weeks of age, but that a decrease becomes evident in more aged $Kir6.2^{-/-}$ mice (21). The result is consistent with the previous study (17) that showed that the total pancreatic insulin content of $GIPR^{-/-}$ mice is lower than that of wild-type ($GIPR^{+/+}$) mice, although the pancreatic β-cell area is increased.

We have shown that the plasma GLP-1 levels are similar in $GIPR^{+/+}$ mice and $GIPR^{-/-}$ mice, and that $GIPR^{-/-}$ mice exhibit higher insulin release in response to GLP-1 (17). These results suggest that the action of GLP-1 is increased in the absence of GIP signaling. Since GLP-1 signaling is still intact in $Kir6.2^{-/-}GIPR^{-/-}$ mice, the increased number of pancreatic β-cells in $Kir6.2^{-/-}GIPR^{-/-}$ mice may be due to the action of GLP-1. These results indicate both that GIP is the major insulinotropic factor in insulin secretion in K_{ATP} channel-deficient mice and that GLP-1 contributes to glucose homeostasis in these mice by stimulating pancreatic β-cell proliferation.

Despite the nearly complete loss of the insulin secretory response to an oral glucose load, $Kir6.2^{-/-}GIPR^{-/-}$ mice still show only mild glucose intolerance. Since GIP receptors are also expressed in the small intestine and in insulin-target tissues such as adipocytes (22), we investigated glucose uptake by the small intestine using everted jejunal rings *in vitro*. Glucose uptake in $Kir6.2^{-/-}GIPR^{-/-}$, $Kir6.2^{-/-}GIPR^{+/+}$, and $Kir6.2^{+/+}GIPR^{+/+}$ mice was similar in this study, suggesting that other factors may contribute to glucose homeostasis in this case, such as increased glucose uptake to adipocytes and skeletal muscle or extrapancreatic glucose-lowering effects of GLP-1 (23).

In the insulin tolerance test, $Kir6.2^{-/-}GIPR^{-/-}$ mice and $Kir6.2^{-/-}GIPR^{+/+}$ mice are similarly insulin sensitive, and more so than $Kir6.2^{+/+}GIPR^{+/+}$ mice. Previous studies have shown that insulin sensitivity is increased by disruption not only of Kir6.2 but also of SUR2, the other component of skeletal muscle K_{ATP} channels. The glucose-lowering effect of insulin, as assessed by the insulin tolerance test, is increased in $Kir6.2^{-/-}$ mice (5), and a 2-deoxy-[^{3}H]glucose uptake experiment *in vivo* has shown that basal and insulin-stimulated glucose uptake in skeletal muscles and adipose tissues of $Kir6.2^{-/-}$ mice is enhanced compared with $Kir6.2^{+/+}$ mice (24). In SUR2-knockout ($SUR2^{-/-}$) mice, enhanced insulin action in skeletal muscle has been reported, and *in vitro* insulin-stimulated glucose transport is 1.5-fold greater than in wild-type ($SUR2^{+/+}$) mice (25). It is thought that K_{ATP} channels consisting of Kir6.2 and SUR2 participate in glucose uptake in skeletal muscles directly while the Kir6.2-containing channels in adipose tissues are involved in glucose uptake only indirectly.

Acknowledgements

We thank Dr T Miki and Prof. S Seino, Chiba University Graduate School of Medicine, Department of Cellular and Molecular Medicine, who provided the $Kir6.2^{-/-}$ mice. This study was supported, in part, by Grants-in-Aids for Scientific Research from the Ministry of Education, Culture, Sports, Science and Technology of Japan, by Health and Labor Sciences Research Grants for Research on Human Genome, Tissue Engineering and Food Biotechnology from the Ministry of Health, Labor and Welfare of Japan, and by Health and Labor Sciences Research Grants for Comprehensive Research on Aging and Health from the Ministry of Health, Labor and Welfare of Japan.

References

1 Ashcroft FM & Rorsman P. Electrophysiology of the pancreatic beta-cell. *Progress in Biophysics and Molecular Biology* 1989 **54** 87–143.
2 Meglasson MD & Matschinsky FM. Pancreatic islet glucose metabolism and regulation of insulin secretion. *Diabetes and Metabolism Reviews* 1986 **2** 163–214.
3 Cook DL, Satin LS, Ashford ML & Hales CN. ATP-sensitive K^+ channels in pancreatic beta-cells. Spare-channel hypothesis. *Diabetes* 1988 **37** 495–498.
4 Misler S, Barnett DW, Gillis KD & Pressel DM. Electrophysiology of stimulus-secretion coupling in human beta-cells. *Diabetes* 1992 **41** 1221–1228.
5 Miki T, Nagashima K, Tashiro F, Kotake K, Yoshitomi H, Tamamoto A, Gonoi T, Iwanaga T, Miyazaki J & Seino S. Defective insulin secretion and enhanced insulin action in K_{ATP} channel-deficient mice. *PNAS* 1998 **95** 10402–10406.
6 Unger RH & Eisentraut AM. Entero-insular axis. *Archives of Internal Medicine* 1969 **123** 261–266.
7 Creutzfeldt W. The incretin concept today. *Diabetologia* 1979 **16** 75–85.

8 Pederson RA, Schubert HE & Brown JC. Gastric inhibitory polypeptide. Its physiologic release and insulinotropic action in the dog. *Diabetes* 1975 **24** 1050–1056.
9 Kashima Y, Miki T, Shibasaki T, Ozaki N, Miyazaki M, Yano H & Seino S. Critical role of cAMP-GEFII–Rim2 complex in incretin-potentiated insulin secretion. *Journal of Biological Chemistry* 2001 **276** 46046–46053.
10 Miyawaki K, Yamada Y, Yano H, Niwa H, Ban N, Ihara Y, Kubota A, Fujimoto S, Kajikawa M, Kuroe A, Tsuda K, Hashimoto H, Yamashita T, Jomori T, Tashiro F, Miyazaki J & Seino Y. Glucose intolerance caused by a defect in the entero-insular axis: a study in gastric inhibitory polypeptide receptor knockout mice. *PNAS* 1999 **96** 14843–14847.
11 Fujimoto S, Ishida H, Kato S, Okamoto Y, Tsuji K, Mizuno N, Ueda S, Mukai E & Seino Y. The novel insulinotropic mechanism of pimobendan: direct enhancement of the exocytotic process of insulin secretory granules by increased Ca^{2+} sensitivity in beta-cells. *Endocrinology* 1998 **139** 1133–1140.
12 Hsu SM, Raine L & Fanger H. A comparative study of the peroxidase-antiperoxidase method and an avidin-biotin complex method for studying polypeptide hormones with radioimmunoassay antibodies. *American Journal of Clinical Pathology* 1981 **75** 734–738.
13 Imagawa K, Nishino T, Shin S, Uehata S, Hashimura E, Yanaihara C & Yanaihara N. Production of anti-glucagon sera with a C-terminal fragment of pancreatic glucagon. *Endocrinologia Japonica* 1979 **26** 123–131.
14 Lostao MP, Urdaneta E, Martinez-Anso E, Barber A & Martinez JA. Presence of leptin receptors in rat small intestine and leptin effect on sugar absorption. *FEBS Letters* 1998 **423** 302–306.
15 Kreymann B, Williams G, Ghatei MA & Bloom SR. Glucagon-like peptide-1 7-36: a physiological incretin in man. *Lancet* 1987 **2** 1300–1304.
16 Scrocchi LA, Brown TJ, MaClusky N, Brubaker PL, Auerbach AB, Joyner AL & Drucker DJ. Glucose intolerance but normal satiety in mice with a null mutation in the glucagon-like peptide 1 receptor gene. *Nature Medicine* 1996 **2** 1254–1258.
17 Pamir N, Lynn FC, Buchan AM, Ehses J, Hinke SA, Pospisilik JA, Miyawaki K, Yamada Y, Seino Y, McIntosh CH & Pederson RA. Glucose-dependent insulinotropic polypeptide receptor null mice exhibit compensatory changes in the enteroinsular axis. *American Journal of Physiology, Endocrinology and Metabolism* 2003 **284** E931–E939.
18 Ling Z, Wu D, Zambre Y, Flamez D, Drucker DJ, Pipeleers DG & Schuit FC. Glucagon-like peptide 1 receptor signaling influences topography of islet cells in mice. *Virchows Archiv* 2001 **438** 382–387.
19 Wettergren A, Schjoldager B, Mortensen PE, Myhre J, Christiansen J & Holst JJ. Truncated GLP-1 (proglucagon 78–107-amide) inhibits gastric and pancreatic functions in man. *Digestive Diseases and Sciences* 1993 **38** 665–673.
20 Navarro M, Rodriquez de Fonseca F, Alvarez E, Chowen JA, Zueco JA, Gomez R, Eng J & Blazquez E. Colocalization of glucagon-like peptide-1 (GLP-1) receptors, glucose transporter GLUT-2, and glucokinase mRNAs in rat hypothalamic cells: evidence for a role of GLP-1 receptor agonists as an inhibitory signal for food and water intake. *Journal of Neurochemistry* 1996 **67** 1982–1991.
21 Miki T, Iwanaga T, Nagashima K, Ihara Y & Seino S. Roles of ATP-sensitive K^+ channels in cell survival and differentiation in the endocrine pancreas. *Diabetes* 2001 **50** (Suppl 1) S48–S51.
22 Miyawaki K, Yamada Y, Ban N, Ihara Y, Tsukiyama K, Zhou H, Fujimoto S, Oku A, Tsuda K, Toyokuni S, Hiai H, Mizunoya W, Fushiki T, Holst JJ, Makino M, Tashita A, Kobara Y, Tsubamoto Y, Jinnouchi T, Jomori T & Seino Y. Inhibition of gastric inhibitory polypeptide signaling prevents obesity. *Nature Medicine* 2002 **8** 738–742.
23 Valverde I, Villanueva-Penacarrillo ML & Malaisse WJ. Pancreatic and extrapancreatic effects of GLP-1. *Diabetes & Metabolism* 2002 **28** 3S85–3S8; discussion 3S108–3S112.
24 Miki T, Minami K, Zhang L, Morita M, Gonoi T, Shiuchi T, Minokoshi Y, Renaud JM & Seino S. ATP-sensitive potassium channels participate in glucose uptake in skeletal muscle and adipose tissue. *American Journal of Physiology, Endocrinology and Metabolism* 2002 **283** E1178–E1184.
25 Chutkow WA, Samuel V, Hansen PA, Pu J, Valdivia CR, Makielski JC & Burant CF. Disruption of Sur2-containing K_{ATP} channels enhances insulin-stimulated glucose uptake in skeletal muscle. *PNAS* 2001 **98** 11760–11764.

Received 16 January 2004
Accepted 16 June 2004

Double Incretin Receptor Knockout (DIRKO) Mice Reveal an Essential Role for the Enteroinsular Axis in Transducing the Glucoregulatory Actions of DPP-IV Inhibitors

Tanya Hansotia,[1] Laurie L. Baggio,[1] Dominique Delmeire,[2] Simon A. Hinke,[2] Yuichiro Yamada,[3] Katsushi Tsukiyama,[3] Yutaka Seino,[3] Jens J. Holst,[4] Frans Schuit,[2] and D.J. Drucker[1]

Glucose-dependent insulinotropic polypeptide (GIP) and glucagon-like peptide 1 (GLP-1) are gut-derived incretins that potentiate glucose clearance following nutrient ingestion. Elimination of incretin receptor action in $GIPR^{-/-}$ or $GLP\text{-}1R^{-/-}$ mice produces only modest impairment in glucose homeostasis, perhaps due to compensatory upregulation of the remaining incretin. We have now studied glucose homeostasis in double incretin receptor knockout (DIRKO) mice. DIRKO mice exhibit normal body weight and fail to exhibit an improved glycemic response after exogenous administration of GIP or the GLP-1R agonist exendin-4. Plasma glucagon and the hypoglycemic response to exogenous insulin were normal in DIRKO mice. Glycemic excursion was abnormally increased and levels of glucose-stimulated insulin secretion were decreased following oral but not intraperitoneal glucose challenge in DIRKO compared with $GIPR^{-/-}$ or $GLP\text{-}1R^{-/-}$ mice. Similarly, glucose-stimulated insulin secretion and the response to forskolin were well preserved in perifused DIRKO islets. Although the dipeptidyl peptidase-IV (DPP-IV) inhibitors valine pyrrolidide (Val-Pyr) and SYR106124 lowered glucose and increased plasma insulin in wild-type and single incretin receptor knockout mice, the glucose-lowering actions of DPP-IV inhibitors were eliminated in DIRKO mice. These findings demonstrate that glucose-stimulated insulin secretion is maintained despite complete absence of both incretin receptors, and they delineate a critical role for incretin receptors as essential downstream targets for the acute glucoregulatory actions of DPP-IV inhibitors. *Diabetes* 53: 1326–1335, 2004

From the [1]Banting and Best Diabetes Centre, Department of Medicine, Toronto General Hospital, University of Toronto, Toronto, Canada; the [2]Molecular Pharmacology Unit, Diabetes Research Center, Faculty of Medicine, Free University of Brussels, Brussels, Belgium; the [3]Department of Diabetes and Clinical Nutrition, Graduate School of Medicine, Kyoto University, Kyoto, Japan; and the [4]Department of Medical Physiology, Panum Institute, Copenhagen, Denmark.

Address correspondence and reprint requests to Daniel J. Drucker, MD, Banting and Best Diabetes Centre, Toronto General Hospital, 200 Elizabeth St., MBRW4R-402, Toronto, Ontario, Canada M5G 2C4. E-mail: d.drucker@utoronto.ca.

Received for publication 25 November 2003 and accepted in revised form 4 February 2004.

F.S. is currently affiliated with the Gene Expression Unit, Afdeling Biochimie, Katholieke Universiteit Leuven, Leuven, Belgium.

D.J.D. has received consulting fees from Merck, Syrrx, and Triad.

DIRKO, double incretin receptor knockout; DPP-IV, dipeptidyl peptidase-IV; GIP, glucose-dependent insulinotropic polypeptide; GLP, glucagon-like peptide 1; Val-Pyr, valine pyrrolidide.

The observation that a glycemic stimulus derived from enteral nutrients exerts a greater insulinotropic response than a comparable isoglycemic challenge achieved through parenteral glucose administration has been termed the incretin effect (1). The first enteroendocrine-derived incretin to be identified, glucose-dependent insulinotropic peptide (GIP), is secreted from duodenal K-cells and rapidly potentiates glucose-dependent insulin secretion (2,3). However, the finding that immunoneutralization of GIP could not completely eliminate the incretin response strongly suggested the existence of additional gut-derived incretins. A second peptide with incretin activity, glucagon-like peptide 1 (GLP-1), was subsequently identified following elucidation of the nucleotide sequence for preproglucagon in the 1980s (4–6).

Human subjects with type 2 diabetes exhibit significant defects in meal-stimulated insulin secretion, leading to the suggestion that diminished incretin action or subnormal incretin secretion may contribute to the pathogenesis of β-cell dysfunction in specific patients (1,7). This hypothesis is supported in part by observations demonstrating resistance to GIP action and reductions in meal-stimulated GLP-1 secretion in diabetic subjects (8,9). The physiological importance of incretin action for glucose control is further illustrated by results of experiments directed at eliminating incretin action in vivo. A combination of peptide antagonists and immunoneutralizing antisera directed against either GIP, GLP-1, or their respective receptors have demonstrated that both GIP and GLP-1 are independently essential for regulation of glucose-dependent insulin secretion (10–12).

A complementary approach for analysis of incretin biology involves the development of mouse models of disrupted incretin receptor action. GIP receptor null mice develop normally and exhibit only modest glucose intolerance following an oral glucose challenge (13,14). Similarly, mice with a null mutation in the GLP-1 receptor gene do not develop severe diabetes but exhibit defective glucose-stimulated insulin secretion and glucose intolerance (15,16). The unexpectedly modest phenotypes of both $GIPR^{-/-}$ and $GLP\text{-}1R^{-/-}$ mice have prompted suggestions that one or more compensatory mechanisms have evolved

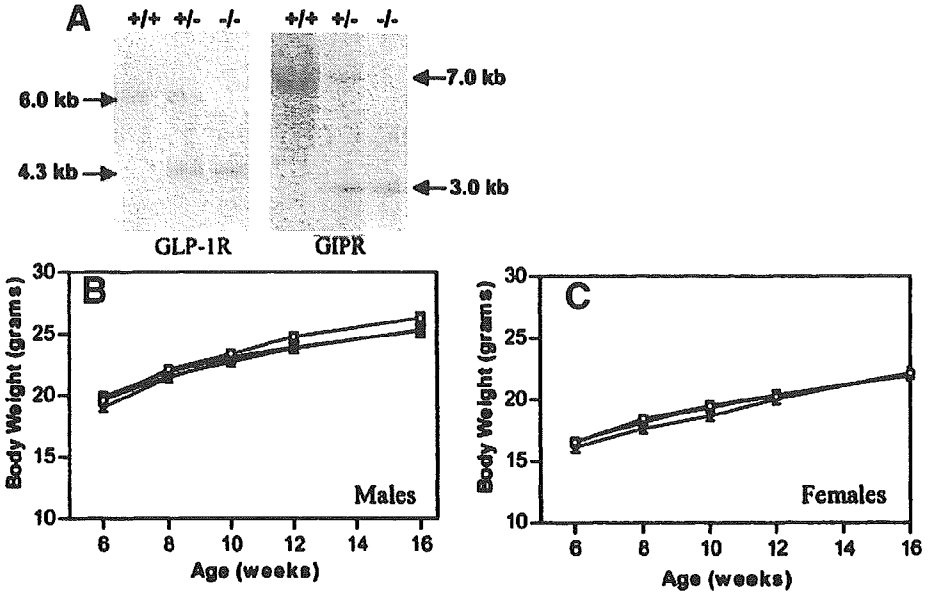

FIG. 1. Genotyping and body weight gain in DIRKO mice. *A*: *Left panel*: *Bam*HI-digested genomic DNA from a GLP-1R$^{+/-}$:GIPR$^{+/-}$ intercross was hybridized with a GLP-1R–specific probe (15). The sizes of the wild-type GLP-1R (6 kb) and targeted allele (4.3 kb) are indicated. *Right panel*: *Eco*RI-digested DNA from a GLP-1R$^{+/-}$:GIPR$^{+/-}$ intercross was hybridized with a GIPR-specific probe. The sizes of the wild-type GIPR (7 kb) and targeted allele (3 kb) are indicated. *B* and *C*: Body weights in male (*B*) and female (*C*) wild-type (○), GIPR$^{-/-}$ (◆), GLP-1R$^{-/-}$ (▲), and DIRKO (■) mice. Body weight (g) was measured at 6, 8, 10, 12, and 16 weeks.

to supplant the role normally subserved by individual incretin receptors in control of glucose homeostasis.

Evidence supporting the upregulation of compensatory mechanisms derives from findings that GLP-1R$^{-/-}$ mice exhibit significantly enhanced β-cell sensitivity to the actions of GIP (17,18), whereas GIPR$^{-/-}$ mice exhibit an enhanced insulin secretory response to GLP-1 (14). Accordingly, we reasoned that the phenotype arising from disruption of single incretin receptor genes in mice may be partially modified as a result of complementary upregulation of the remaining intact incretin receptor axis. To identify the essential roles of GIP and GLP-1 for glucose homeostasis and to determine whether incretin receptors are key downstream targets essential for the action of dipeptidyl peptidase-IV (DPP-IV) inhibitors, we have now generated and characterized double incretin receptor knockout (DIRKO) mice with complete loss of both GIP and GLP-1 receptor action.

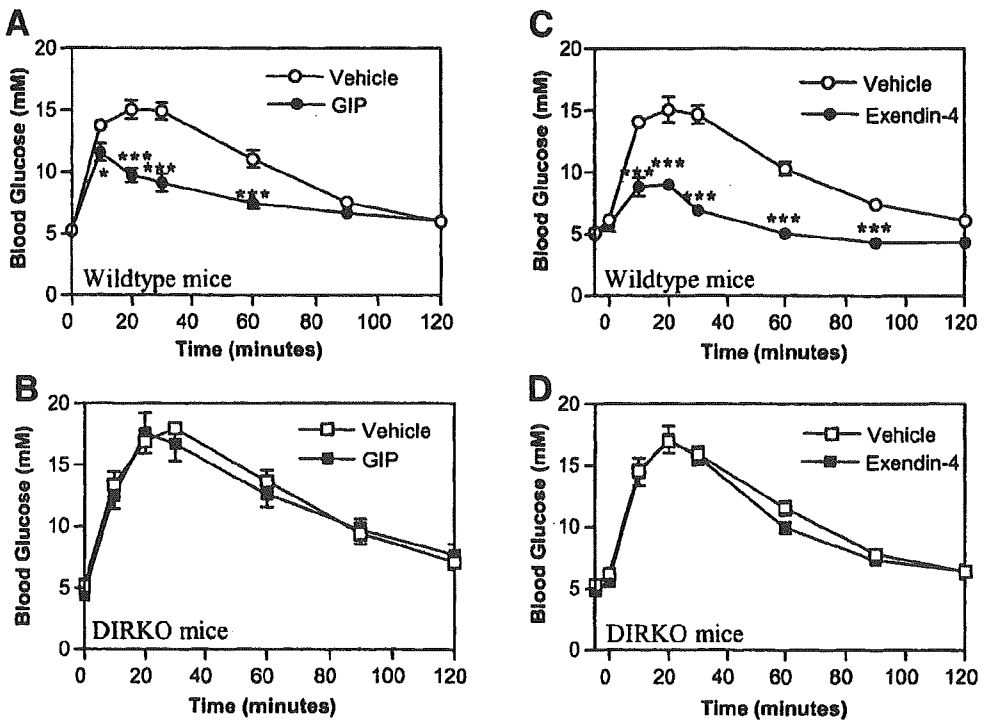

FIG. 2. GIP and exendin-4 lower glucose in wild-type mice but not in DIRKO mice. Blood glucose levels during oral glucose tolerance test in wild-type (*A* and *C*) and DIRKO (*B* and *D*) mice following administration of GIP (50 μg) or vehicle (saline). Administration of exendin-4 (100 ng) or saline to wild-type (*C*) and DIRKO (*D*) mice. Values are expressed as means ± SE; n = 3–7 mice/group. *$P < 0.05$ and ***$P < 0.001$, peptide vs. vehicle-treated mice.

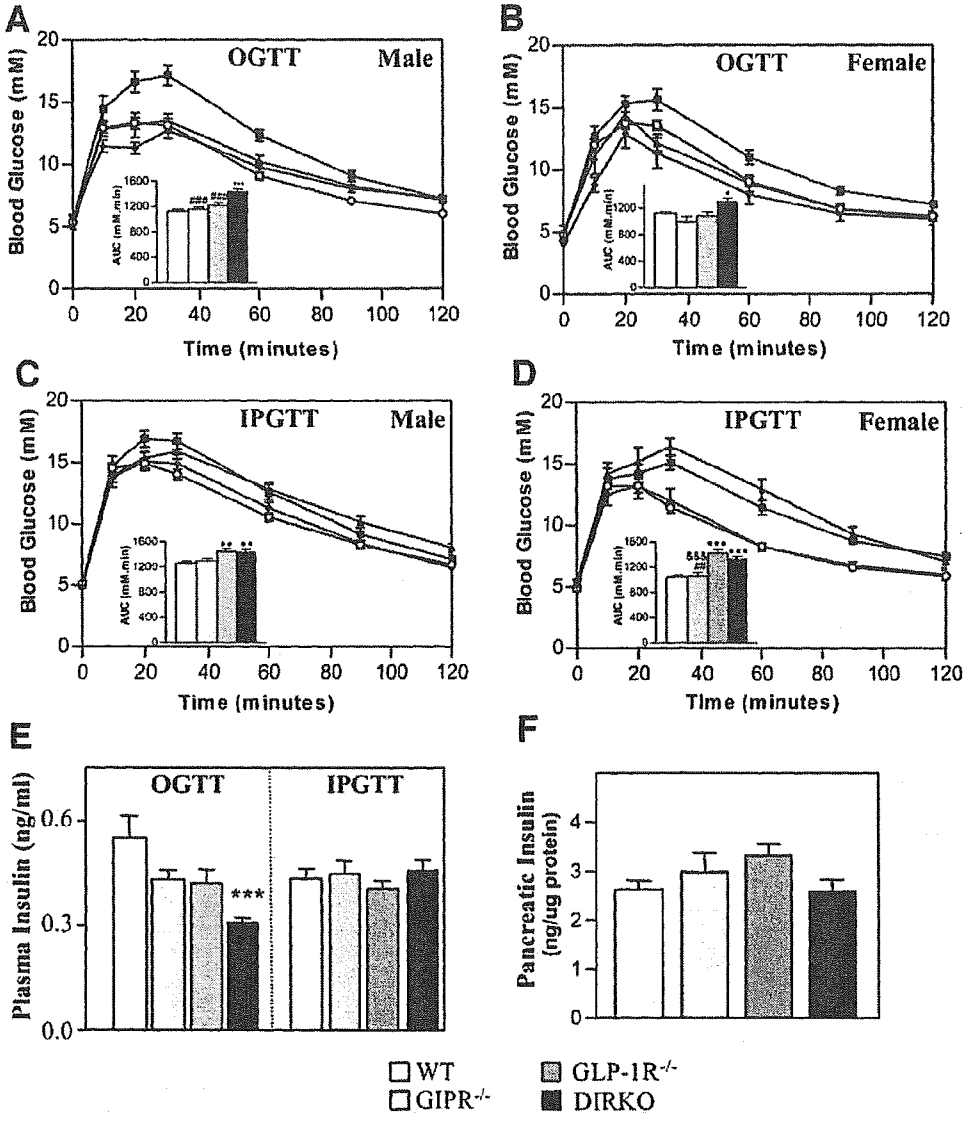

FIG. 3. Oral glucose tolerance and intraperitoneal glucose tolerance and plasma insulin in wild-type, GIPR$^{-/-}$, GLP-1R$^{-/-}$, and DIRKO mice. ***A*** **and** ***B*****: Oral glucose tolerance in male (*A*; *n* = 13–28 mice/group) and female (*B*, *n* = 4–14 mice/group) wild-type (○), GIPR$^{-/-}$ (◆), GLP-1R$^{-/-}$ (▲), and DIRKO (■) mice.** ***C*** **and** ***D*****: Intraperitoneal glucose tolerance in male (*C*) (*n* = 16–29 mice/group) and female (*D*) (*n* = 6–14 mice/group) wild-type (○), GIPR$^{-/-}$ (◆), GLP-1R$^{-/-}$ (▲), and DIRKO (■) mice. For *A–D*, insets depict quantification of the area under the curve for total glycemic excursions.** ***E*****: Plasma insulin concentrations, measured in plasma obtained 10 min after glucose administration, following oral or intraperitoneal glucose tolerance in wild-type (WT), GIPR$^{-/-}$, GLP-1R$^{-/-}$, and DIRKO male mice (*n* = 6–14 mice/group).** ***F*****: Pancreatic insulin content in fasted wild-type, GIPR$^{-/-}$, GLP-1R$^{-/-}$, and DIRKO male mice.** ***G*****: Islet histology and insulin immunostaining of islets in wild-type and DIRKO mice. Magnification = 40 and 400× for different photomicrographs shown.** ***H*****: Plasma levels of glucagon in the fasting state and during oral glucose challenge in wild-type, GIPR$^{-/-}$, GLP-1R$^{-/-}$, and DIRKO mice. Values are expressed as means ± SE; *n* = 4–9 mice/group. *P < 0.05, **P < 0.01, and ***P < 0.001 vs. wild-type mice; &&&P < 0.001 vs. GLP-1R−/−; ##P < 0.01 and ###P < 0.001 vs. DIRKO mice. IPGTT, intraperitoneal glucose tolerance test; OGTT, oral glucose tolerance test.**

RESEARCH DESIGN AND METHODS

Generation of GLP-1R$^{-/-}$:GIPR$^{-/-}$ (DIRKO) mice. As GIP receptor mice were generated in the C57BL/6 background (13), whereas GLP-1R$^{-/-}$ mice were originally derived in the CD1 background (15), we first backcrossed GLP-1R$^{-/-}$ mice for five generations into the C57BL/6 background. The GIPR$^{-/-}$ mice were then crossed with the GLP-1R$^{-/-}$ mice on the same C57BL/6 background. The subsequent heterozygotes were crossed to generate GLP-1R$^{-/-}$:GIPR$^{-/-}$ mice. All mice used in these studies were 9–15 weeks of age. Single and double incretin receptor knockout mice and age and sex-matched control C57BL/6 wild-type mice (Charles River, Montreal, PQ) were housed under a light/dark cycle of 12 h in the Toronto General Hospital Animal facility with free access to food (standard rodent diet) and water, except where noted. All wild-type mice used for these studies were acclimatized to the animal facility for several weeks before analysis. All procedures were conducted according to protocols and guidelines approved by the Toronto General Hospital and Vrije Universiteit Brussel animal care committees. For confirmation of genotypes, genomic DNA prepared from tail snips was analyzed by Southern blotting (16).

Glucose tolerance tests and measurement of plasma insulin. Oral or intraperitoneal glucose tolerance tests were carried out following an overnight fast (16–18 h) as described (11). Mice were given 1.5 mg glucose/g body wt through a gavage tube (oral glucose tolerance test) or via injection into the peritoneal cavity (intraperitoneal glucose tolerance test). Peptide administration was via the intraperitoneal route. GIP (California Peptide Research, Napa, CA) and exendin-4 (California Peptide Research) were injected immediately before glucose loading at a dose of 50 μg (GIP) or 100 ng (exendin-4) per mouse, respectively.

Studies with DPP-IV inhibitors. For analysis of the effects of DPP-IV inhibitors, mice were injected intraperitoneally with valine pyrrolidide (Val-Pyr; Merck Research Laboratories, Rahway, NJ) at a dose of 30 mg/kg body wt

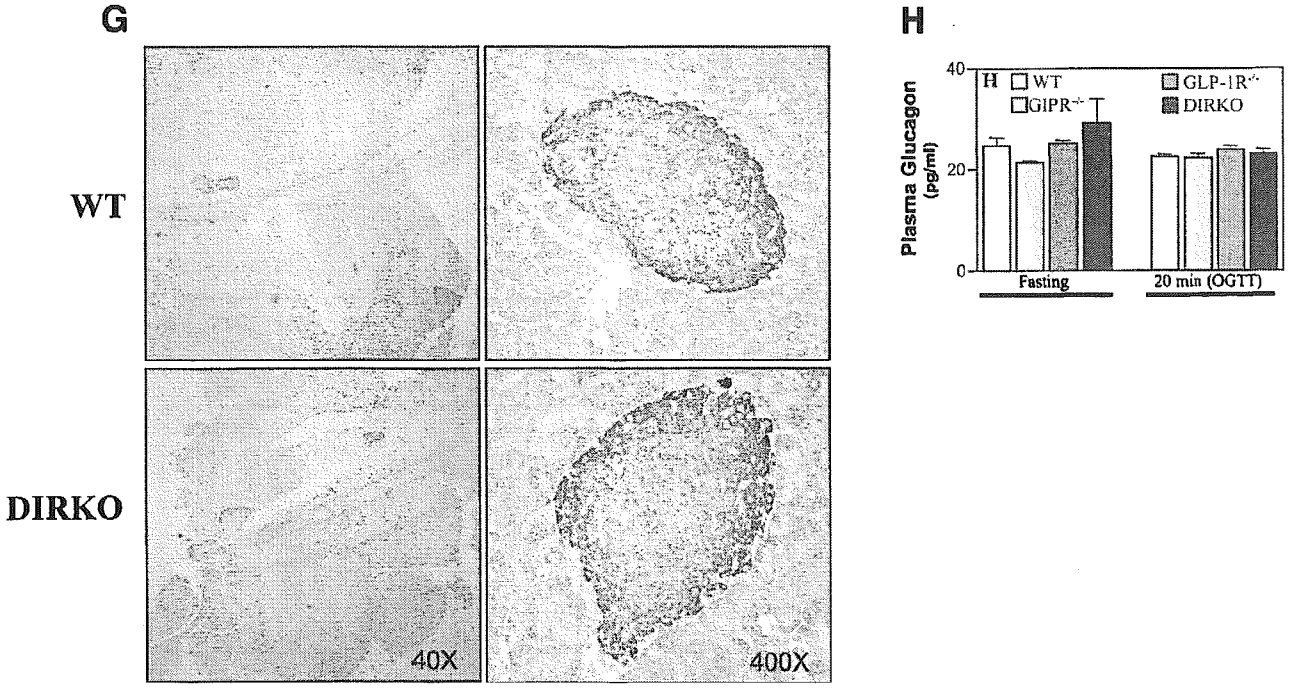

FIG. 3—*Continued.*

or the same volume of vehicle (H_2O) 30 min before glucose administration. For studies with Syrrx 106124 (Syrrx, La Jolla, CA), the compound was administered orally 60 min before glucose challenge at a dose of 10 mg/kg body wt; the same volume of vehicle (H_2O) alone was administered as a control. LAF237 was obtained from Novartis Pharmaceuticals (East Hanover, NJ) and was given orally 20 min before an oral glucose challenge at a dose of 5 mg/kg body wt. TP8211 was obtained from Dr. W. Bachovchin, Tufts University (Boston, MA) and was administered 60 min before an oral glucose challenge at a dose of 2.5 and 12.5 mg/kg body wt. Blood was drawn from a tail vein at 0, 10, 20, 30, 60, 90, and 120 min following glucose administration, and blood glucose levels were measured by the glucose oxidase method using a One Touch Basic Glucometer (Lifescan, Burnaby, BC, Canada). Blood samples (100 μl) for measurement of plasma insulin were removed from a tail vein during the 10- to 20-min time period following oral or intraperitoneal glucose administration. Plasma was assayed for insulin using a rat insulin enzyme-linked immunosorbent assay kit (Crystal Chem, Chicago, IL) with mouse insulin as a standard (11).

Islet isolation and perifusion. The pancreatic islets of Langerhans were isolated from overnight fasted 11- to 15-week old male and female C57BL/6 and DIRKO mice by collagenase digestion and hand picked under dissection microscopes as described (16,18). Islets from wild-type and knockout mice were immediately perifused in parallel (100 islets/chamber), using pH 7.4 Ham's F10 media (Gibco) supplemented with 15 mmol/l HEPES (Sigma), 0.5% BSA (Boehringer Mannheim), 2 mmol/l glutamine (Gibco), and 2 mmol/l Ca^{2+}, with varied glucose concentrations. Perifusion media was bubbled with carbogen (95% O_2/5% CO_2) to ensure adequate oxygen tension and pH stability. Chambers were perifused at a rate of 0.5 ml/min, and samples were taken each minute. The perifusion protocol consisted of 30 min of basal 1 mmol/l glucose perifusate followed by stepwise increases in glucose concentration (5, 8, 11, and 20 mmol/l; 10 min/step). Following this protocol, islets were perifused for 10 min each with 20 mmol/l glucose + 10 nmol/l GLP-1 + 10 nmol/l GIP and then 20 mmol/l glucose + 3 μmol/l forskolin + 0.1 mmol/l IBMX (peptides and compounds from Sigma), allowing islets to return to baseline secretory levels (by 15 min) between each test. At the end of the protocol, islet insulin content was determined by sonicating islets in 0.25% BSA with 2 mol/l acetic acid, followed by radioimmunoassays as described (16,18). Insulin secretion was measured in each fraction by radioimmunoassay and expressed as a percent of total cell content (16,18). Pancreatic insulin content was measured after an overnight fast as described previously (19).

Measurement of plasma glucagon, GLP-1, and GIP. Mice were killed after an overnight fast or 20 min following administration of oral glucose (1.5 mg glucose/g body wt). Mice were anesthetized with CO_2, and blood samples were collected by cardiac puncture and mixed with 10% (vol/vol) TED (500,000 KIU/m Trasylol, 1.2 mg/ml EDTA, and 0.1 mmol/l Diprotin A). The plasma was separated by centrifugation at 4°C and stored at −80°C. Plasma glucagon was measured using a glucagon radioimmunoassay kit (Linco Research, St. Louis, MO). GIP and GLP-1 concentrations in plasma were measured after extraction of plasma with 70% ethanol (vol/vol, final concentration). For the GIP radioimmunoassay (20,21), we used the COOH-terminally directed antiserum R 65, which cross-reacts fully with murine GIP and with GIP (3-42), but not with larger forms of GIP. Human GIP and [^{125}I] human GIP (70 MBq/nmol) were used for standards and tracer. The plasma concentrations of GLP-1 were measured (22) against standards of synthetic GLP-1(7-36^{amide}) using antiserum code no. 89390, which is specific for the amidated COOH-terminus of GLP-1 and does not react with GLP-1–containing peptides from the pancreas. The assay measures the sum of intact GLP-1 and the primary metabolite, GLP-1(9-36^{amide}). For both assays, sensitivity was <1 pmol/l, intraassay coefficient of variation was <6% at 20 pmol/l, and recovery of standard, added to plasma before extraction, was almost 100% when corrected for losses inherent in the plasma extraction procedure.

Insulin tolerance test. Wild-type and DIRKO mice were fasted for 5 h and given 1.7 units/kg insulin (Humulin R, 100 units/ml; Lilly, Toronto, ON) by intraperitoneal injection. Blood glucose was monitored for 4 h after the insulin challenge.

Histology and immunohistochemistry. The pancreas was removed, fixed overnight in 5% glacial acetic acid/25% formaldehyde (vol/vol), and embedded in paraffin. Sections were obtained and stained with hematoxylin and eosin using standard protocols. Immunostaining for insulin was carried out as previously described (19,23).

Statistics. Results are expressed as means ± SE. Statistical significance was assessed by one-way and two-way ANOVA and, where appropriate, a Student's *t* test using GraphPad Prism 3 (GraphPad Software, San Diego, CA). A P value of <0.05 was considered to be statistically significant.

RESULTS

GIPR$^{-/-}$ and GLP-1R$^{-/-}$ mice were crossed (Fig. 1*A*) to generate DIRKO mice. Transmission of the mutant alleles was confirmed by Southern blotting (Fig. 1*A*). DIRKO mice were viable and fertile, appeared normal, and exhibited no disturbances in growth (Fig. 1*B* and *C*). Analysis of food intake over a 24-h time period revealed small but significant increases in food intake at some time points in DIRKO and GLP-1R$^{-/-}$ but not in GIPR$^{-/-}$ mice, consistent with our previous studies of food intake in GLP-1R$^{-/-}$ mice in the CD1 background (15,24,25). In view of reports

continuing to suggest evidence for a second functional GLP-1R and to verify the functional absence of responses to exogenous incretins, we administered either the GLP-1R agonist exendin-4 or GIP to glucose-loaded wild-type and DIRKO mice. GIP and exendin-4 significantly reduced glycemic excursion following glucose challenge in wild-type mice; however, these peptides had no glucose-lowering effect in DIRKO mice (Fig. 2). Hence, combined targeted disruption of the two established incretin receptors completely eliminates the glucose-lowering effects of GIP and GLP-1 receptor agonists in mice.

In agreement with the presumed physiological importance of GIP and GLP-1, $GIPR^{-/-}$ and $GLP\text{-}1R^{-/-}$ mice exhibited glucose intolerance following oral glucose challenge. In contrast, fasting glucose was significantly elevated in $GLP\text{-}1R^{-/-}$ in the CD1 background, but not in $GIPR^{-/-}$ mice (13,15). Fasting glucose was not significantly elevated in DIRKO mice (Figs. 2 and 3). Nevertheless, glycemic excursion was abnormally increased following oral glucose administration to DIRKO relative to wild-type mice or to mice lacking a single incretin receptor (Fig. 3*A* and *B*). Furthermore, the levels of glucose-stimulated plasma insulin were lower in $GIPR^{-/-}$ and $GLP\text{-}1R^{-/-}$ mice following oral glucose challenge and were significantly reduced in DIRKO mice relative to levels in wild-type mice (Fig. 3*E*). In contrast, glycemic excursion following intraperitoneal glucose challenge was abnormally increased in DIRKO relative to wild-type mice but was not significantly different compared with excursion profiles seen with $GLP\text{-}1R^{-/-}$ mice (Fig. 3*C* and *D*). A trend toward sexual dimorphism was observed, with $GLP\text{-}1R^{-/-}$ and DIRKO females being comparatively more glucose intolerant to an intraperitoneal glucose load than their male counterparts (Fig. 3*C* and *D*). Furthermore, no significant difference was detected in levels of glucose-stimulated plasma insulin in single incretin receptor knockout versus DIRKO mice following intraperitoneal glucose loading (Fig. 3*E*). Moreover, total pancreatic insulin content measured in the fasted state was normal in DIRKO mice (Fig. 3*F*), and no apparent difference in the number and size of DIRKO versus wild-type islets was observed (Fig. 3*G*). Mean levels of GIP were similar in fasted wild-type and DIRKO mice (8.3 ± 0.8 vs. 6.2 ± 0.8 pmol/l, respectively). In contrast, following oral glucose challenge, the levels of circulating GIP were significantly higher in wild-type compared with DIRKO mice (34.4 ± 5.6 vs. 12.6 ± 2.0 pmol/l, respectively, $P < 0.05$). In contrast, circulating levels of GLP-1 were lower in DIRKO mice in both the fasted state and following glucose challenge (17.2 ± 1.0 vs. 12.1 ± 1.7 pmol/l and 28.5 ± 0.5 vs. 11.5 ± 2.5 pmol/l, wild-type vs. DIRKO mice, respectively).

To determine whether the perturbations in glycemic excursion detected in DIRKO mice reflected compensatory changes in sensitivity to insulin, we compared the acute glycemic response to exogenous insulin in wild-type versus DIRKO mice. No differences were observed in the magnitude of glucose reduction or the recovery from insulin-induced hypoglycemia in wild-type versus DIRKO mice (data not shown). Similarly, although both GLP-1 and GIP are known regulators of plasma glucagon secretion (26,27), no significant differences (wild-type versus single incretin receptor knockout versus DIRKO mice) were observed in the levels of plasma glucagon in the fasting state or following oral glucose administration (Fig. 3*H*).

The modest impairment in glucose-stimulated insulin secretion observed in DIRKO mice prompted us to assess whether potential compensatory factors upregulating β-cell secretory function might be revealed by analysis of glucose-stimulated insulin secretion in isolated DIRKO islets. The dynamic secretion of insulin by freshly isolated islets is shown in Fig. 4. By stepwise increases in glucose concentration in the perifusate, it was possible to plot concentration response curves for assessment of islet sensitivity to glucose. The perifusion profiles (Fig. 4*A* and *B*), comparing wild-type with DIRKO mice and separating results by sex, indicated that islets from either sex respond similarly to glucose. A trend toward sexual dimorphism was observed between male and female DIRKO mice, with males being more responsive to glucose than females (Fig. 4*A* and *B*). Comparison of the integrated insulin responses showed that the male DIRKO mice were more responsive than both male wild-type and female DIRKO animals at the step from 11–20 mmol/l glucose ($P < 0.05$). However, calculation of the initial secretion rate (average of the peak two to three tubes immediately following the change in glucose concentration) or the "plateau" secretion rate (average of the last three tubes before changing perifusate glucose concentration) indicated that the male DIRKO islets showed normal secretion kinetics; in contrast, although the sensitivity of female DIRKO islets to glucose was preserved, their secretion kinetics showed a trend (not statistically significant) toward impairment.

While freshly isolated islets are commonly used for study of responsiveness to glucose and direct activators of signal transduction cascades (28), the acute secretory response to hormones may be blunted, likely due to receptor damage by collagenase (29). Nevertheless, both GIP and GLP-1 acutely stimulated insulin secretion immediately following islet isolation (~20% increase) from wild-type but not DIRKO islets, and perifusion following overnight islet culture confirmed a complete lack of responsiveness to each incretin alone in islets from DIRKO mice (data not shown). Comparing the integrated insulin secretory responses obtained with either GIP or GLP-1, either incretin was able to account for a difference of 80–90% of the insulin response between wild-type and DIRKO islets (data not shown).

To confirm retention of islet secretory capacity at the conclusion of the perifusion studies, islets were perifused for 10 min with the phosphodiesterase inhibitor (IBMX; 0.1 mmol/l) and forskolin (3 μmol/l), a direct activator of adenylyl cyclase. Figure 4*E* shows the integrated insulin responses to 20 mmol/l glucose alone or with forskolin/IBMX for both male and female wild-type and DIRKO islets. Activation of the cAMP pathway resulted in similar amplification of insulin secretion for all mice ($P > 0.05$). These findings confirmed the viability of the islets for the duration of the perifusion protocol and demonstrate that genetic removal of both incretin receptors does not impair responsiveness to second messenger systems coupled to incretin receptor activation. It is also noteworthy that another sexual dimorphism was observed, independent of the genetic disruption of the incretin receptors. Both

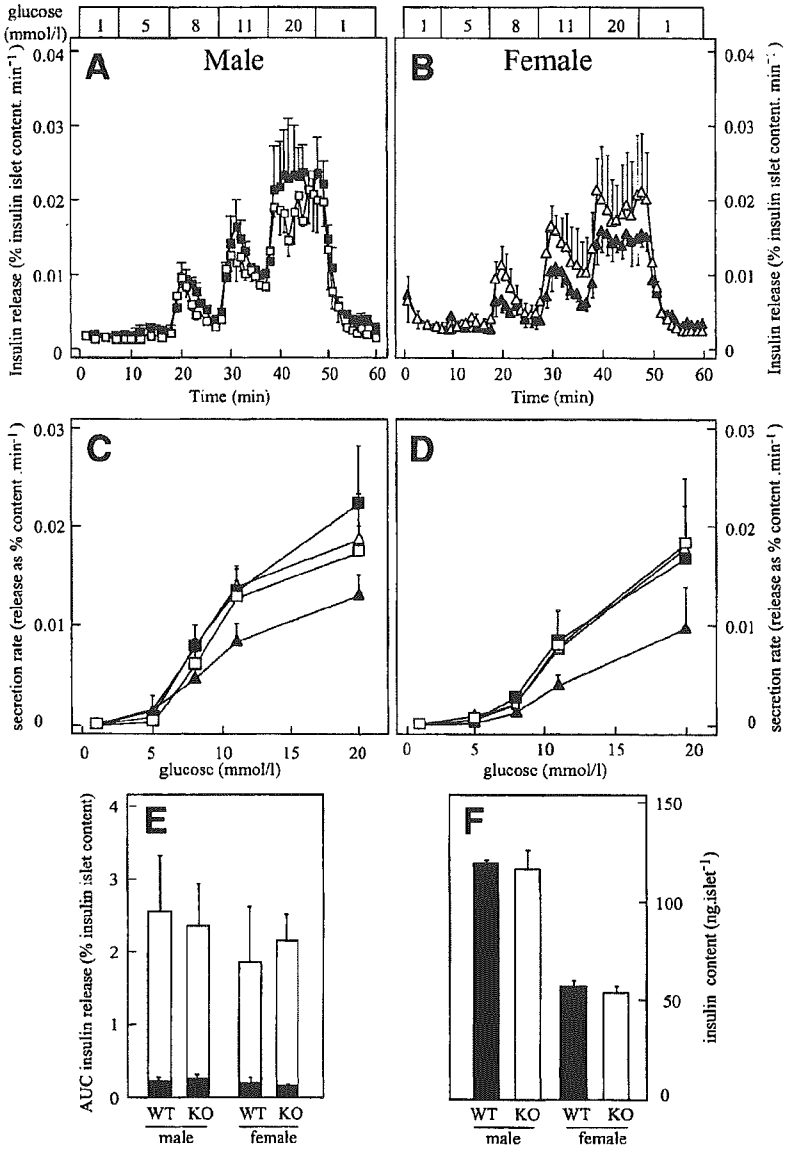

FIG. 4. Insulin release and content from C57BL/6 and DIRKO mouse islets. Islets from male (squares, *A*) and female (triangles, *B*) C57BL/6 wild-type mice (open) and DIRKO mice (closed) were perifused immediately following isolation with basal medium (1 mmol/l glucose) and tested for their insulin-releasing capacity in response to increasing glucose concentrations (*A–D*: 5–20 mmol/l glucose) (n = 3 mice per group). *C*: First-phase insulin secretion rate (min 1–3) with specific perifusion stimuli shown in *A* and *B*. *D*: Average plateau secretion rate (min 8–10) with stimuli shown in *A* and *B*. *E*: As a positive control, the islets were finally perifused with 3 μmol/l forskolin combined with 0.1 mmol/l IBMX at 20 mmol/l glucose. The open bars represent area under the curve (AUC) of the insulin-releasing capacity to 3 μmol/l forskolin combined with 0.1 mmol/l IBMX and 20 mmol/l glucose. The solid bars depict the AUC insulin-releasing capacity in response to 20 mmol/l glucose alone. *F*: Insulin content (ng/islet) in wild-type (WT) and DIRKO (KO) mice.

wild-type and DIRKO female mice contained ~50% of the islet insulin content of their male counterparts (Fig. 4*F*; $P < 0.05$). The underlying reason for this finding remains unclear; however, the amount of insulin released as a percentage of total cell content was not altered in wild-type mice, regardless of sex.

Activation of incretin receptor pathways by enhancing endogenous levels of GLP-1 and GIP contributes to the glucose-lowering activity of DPP-IV inhibitors (30). DPP-IV is the key enzyme responsible for inactivating both GLP-1 and GIP, and genetic disruption or pharmacological inhibition of DPP-IV lowers blood glucose in rodent and human studies (31,32). DPP-IV inhibitors modify the activity of multiple peptide substrates with glucose-lowering effects in addition to GIP and GLP-1 (33–35). Accordingly, we examined the activity of DPP-IV inhibitors in mice with single and combined genetic disruption of incretin receptor action. The DPP-IV inhibitor Val-Pyr significantly reduced glycemic excursion following oral glucose challenge in association with increased levels of plasma insulin not only in wild-type mice (Fig. 5*A*), but also in GLP-1R$^{-/-}$ and GIPR$^{-/-}$ mice (Fig. 5*B* and *C*). In contrast, Val-Pyr had no effect on plasma insulin or glucose in DIRKO mice (Fig. 5*D*). To ascertain that the elimination of glucose lowering with Val-Pyr did not represent a compound-specific effect, we assessed glucose excursion following administration of SYR106124, a structurally different DPP-IV inhibitor. Although SYR106124 reduced glycemia and increased levels of plasma insulin following glucose loading in wild-type mice (Fig. 6*A* and *B*), SYR106124 had no effect on blood glucose or insulin in DIRKO mice (Fig. 6*C* and *D*). Similarly, two additional structurally distinct DPP-IV inhibitors, TP8211 and LAF237, significantly lowered glucose in wild-type but not in DIRKO mice (data not shown). Taken together, these findings demonstrate that functional incretin receptors represent essential downstream targets for transducing the acute glucose-lowering effects of DPP-IV inhibitors.

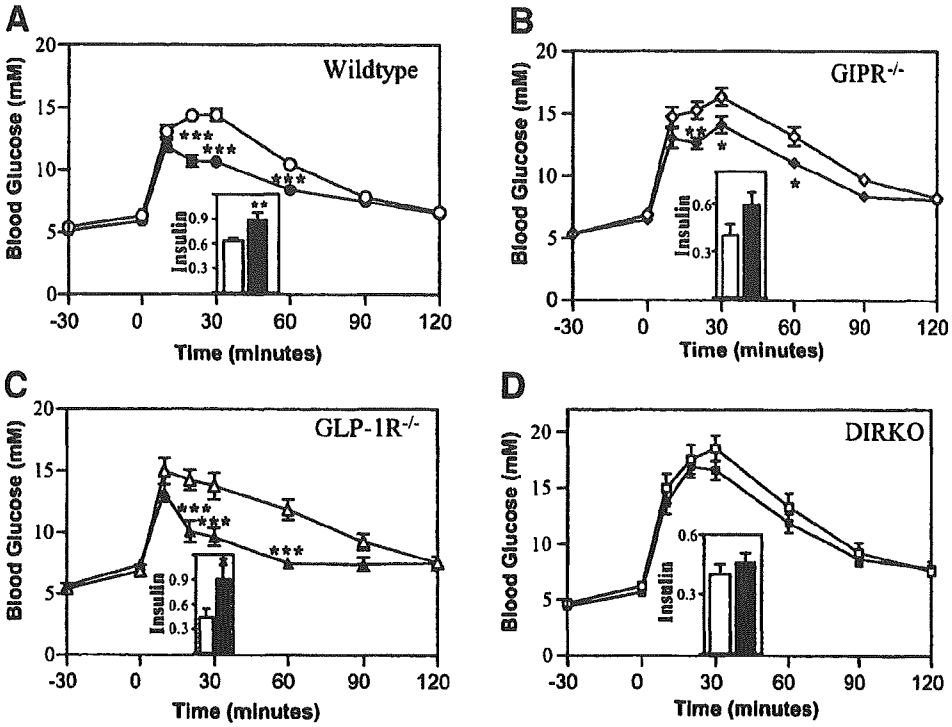

FIG. 5. The DPP-IV inhibitor Val-Pyr fails to lower blood glucose in DIRKO mice. Male mice were given intraperitoneal injections of vehicle (H_2O) or 30 mg/kg Val-Pyr 30 min before oral glucose loading. Oral glucose tolerance following administration of either vehicle (open symbols) or Val-Pyr (solid symbols) to wild-type (*A*), $GIPR^{-/-}$ (*B*), $GLP\text{-}1R^{-/-}$ (*C*), and DIRKO (*D*) mice (n = 6–14 mice/group). Plasma insulin levels (ng/ml) were determined in samples obtained 10 min after oral glucose challenge are shown as insets (n = 4–11 mice/group). Values are expressed as means ± SE. $^*P < 0.05$, $^{**}P < 0.01$, and $^{***}P < 0.001$ vehicle vs. Val-Pyr–treated mice.

DISCUSSION

The enteroinsular axis, a term coined by Unger and Eisentraut (36), describes the phenomena of greater insulin release when nutrients are taken orally versus intravenously, even if glycemic conditions are matched (37,38). Consistent with the importance of GIP and GLP-1 for function of the enteroinsular axis, mice lacking either GLP-1 or GIP receptors exhibit defective glucose-stimu-

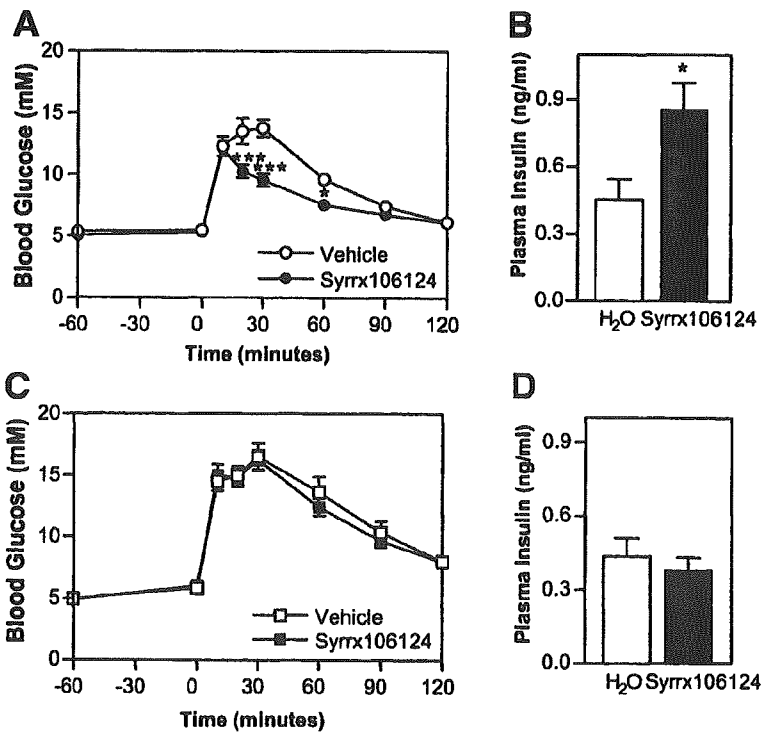

FIG. 6. Administration of Syrrx106124 improves glucose tolerance in wild-type but not in DIRKO mice. Vehicle (H_2O) or 10 mg/kg Syrrx106124 was administered 60 min before oral glucose loading. Oral glucose tolerance testing was carried out following oral administration of vehicle or Syrrx106124 to wild-type (*A*) and DIRKO (*C*) mice (n = 10–13 mice/group). Plasma insulin levels were determined in samples obtained 10 min after oral glucose administration in wild-type (*B*) and DIRKO (*D*) mice (n = 5–8 mice/group). Values are expressed as means ± SE. $^*P < 0.05$ and $^{***}P < 0.001$ vehicle vs. Syrrx101624-treated mice.

lated insulin secretion (13–15,39). Surprisingly, however, glucose intolerance in mice with disruption of single incretin receptor genes is relatively modest and thought to be due in part to compensatory upregulation of the remaining functionally intact incretin receptor axis (14,17). Accordingly, we reasoned that inactivation of both incretin receptor genes in a single mouse would substantially impair glucose tolerance, further illustrating the essential roles of incretin receptor action in glucose homeostasis.

DIRKO mice exhibit significantly greater glucose intolerance following oral glucose challenge than mice with genetic inactivation of a single incretin receptor gene. Furthermore, despite the potential for multiple complementary actions (effects on glucagon and gastric emptying) of GLP-1 to complicate interpretation of the effects of incretin receptor disruption on the β-cell, the increased glycemic excursion following oral glucose challenge in DIRKO mice was associated with inappropriately reduced levels of plasma insulin. These data strongly affirm the importance of incretin receptor signaling for β-cell function after enteral nutrient administration. Surprisingly, however, fasting glucose was normal and levels of glucose-stimulated insulin were not significantly different in wild-type versus DIRKO mice following IPGTT, consistent with the absence of a severe generalized β-cell defect in DIRKO islets. The preservation of β-cell function in DIRKO mice was not likely due to enhanced GIP or GLP-1 action through novel incretin receptors, as no changes in plasma glucose were observed following pharmacological GIP or exendin-4 administration.

Our previous studies of GLP-1R$^{-/-}$ mice revealed evidence for mild fasting hyperglycemia (15), whereas fasting glucose was normal in GLP-1R$^{-/-}$ mice studied here, as well as in the DIRKO mouse. Furthermore, we previously described a modest but significant reduction in pancreatic insulin content in GLP-1R$^{-/-}$ mice (17), whereas pancreatic insulin content was normal in both the DIRKO and GLP-1R$^{-/-}$ pancreas in the present studies. One important potential explanation for the variations in phenotypes observed in GLP-1R$^{-/-}$ mice is the different genetic backgrounds of these mice. Our previous studies describing characterization of the GLP-1R$^{-/-}$ mouse were obtained in experiments analyzing the GLP-1R null mutation in the CD1 background (15–17,39). In contrast, the data obtained in our current study represent the first analysis of the phenotype of the GLP-1R null mutation in the C57BL/6 background. Given the potential importance of even minor strain variation on phenotypes related to glucose homeostasis (40), we cannot exclude the possibility that one or more subtle differences in phenotypic characterization of the current GLP-1R$^{-/-}$ mouse is related to the new genetic background.

The classic definition of the enteroinsular axis invokes a comparatively greater release of insulin following oral versus parenteral glucose challenge (1). Indeed, wild-type mice clearly exhibit greater levels of plasma insulin following oral versus intraperitoneal glucose loading (Fig. 3). In contrast, the incretin effect is eliminated in mice with a single disrupted incretin receptor gene, and levels of plasma insulin are paradoxically lower in DIRKO mice after oral versus intraperitoneal glucose administration. Surprisingly, however, DIRKO islets maintain relatively normal glucose-induced insulin secretion in vitro. Previous studies have shown that exposure of murine β-cells to the GLP-1R antagonist exendin (9-39) reduces levels of cAMP and glucose-stimulated insulin secretion, implying that constitutive GLP-1 receptor signaling is essential for stimulus secretion coupling in the β-cell (18,41). Nevertheless, the relative preservation of glucose-stimulated insulin secretion in perifused islets, the normal fasting glucose, taken together with the comparatively well-preserved response to intraperitoneal glucose, suggests that DIRKO islets may have evolved as yet unidentified compensatory mechanisms that mask the functional absence of the GIP and GLP-1 receptors. Furthermore, it appears that additional defects in the secretory response of DIRKO islets may be unmasked following incubation of islets for varying periods of time in nutrient-depleted medium (B. Thorens, unpublished observations).

Although the GLP-1 and GIP receptors are viewed as important modulators of β-cell signal transduction and glucose-stimulated insulin secretion, the DIRKO β-cell seems likely to have adapted to the genetic absence of incretin receptors via upregulation of related compensatory signaling systems. For example, PACAP receptors are expressed on islet β-cells, and genetic disruption of the PAC1 receptor in mice results in reduction of glucose-stimulated insulin secretion in mice in vivo and in intact islets in vitro (42). Similarly, glucagon is a potent activator of cyclic AMP formation and insulin secretion (43), and studies using a specific glucagon receptor antagonist (44) reveal an essential role for the β-cell glucagon receptor as an important regulator of glucose-stimulated insulin secretion. Hence, it remains possible that the comparatively intact β-cell function observed in the DIRKO mouse reflects enhanced sensitivity to functionally related peptides with insulinotropic activity and/or upregulation of downstream signaling molecules that contribute to the maintenance of appropriate glucose-stimulated insulin secretion.

The increasing interest in the evaluation of DPP-IV inhibitors for the treatment of subjects with type 2 diabetes (45,46) prompted us to assess whether incretin receptors are essential for DPP-IV inhibitor action. Although multiple regulatory peptides, including GIP, are known substrates for DPP-IV (47), current concepts invoke GLP-1 as the principal mediator of DPP-IV inhibitor–associated reduction in blood glucose (46, 48). Nevertheless, some studies examining the glucose-lowering properties of DPP-IV inhibitors demonstrate more pronounced effects on stabilization of plasma GIP compared with GLP-1. Moreover, previous studies have shown that the GLP-1R is not essential for DPP-IV inhibitor action, as Val-Pyr lowered blood glucose and stimulated insulin secretion in mice with complete absence of GLP-1R activity (31). Accordingly, the relative importance of GIP and GLP-1 as targets for the actions of DPP-IV inhibitors remains uncertain.

We demonstrate here that Val-Pyr not only reduces glycemic excursion in GLP-1R$^{-/-}$ mice, but also lowers blood glucose in GIPR$^{-/-}$ mice. One possible explanation for these findings lies in the broad substrate specificity of DPP-IV (47). For example, pituitary adenylate cyclase–activating peptide, bradykinin, gastrin-releasing peptide, and GIP are known DPP-IV substrates and exert glucose-lowering effects in vivo (33–35,49). In preliminary studies

using smaller numbers of mice, we initially detected a small reduction in blood glucose using Val-Pyr in DIRKO mice (50). In contrast, our studies described here using larger numbers of mice and a panel of different DPP-IV inhibitors demonstrate that the acute glucose-lowering effects of these compounds are absent in DIRKO mice. Our findings that multiple structurally distinct DPP-IV inhibitors have no acute effect on blood glucose or plasma insulin in DIRKO mice strongly suggest that the GLP-1 and GIP receptors are the principal targets essential for the acute glucose-lowering actions of DPP-IV inhibitors.

Nevertheless, our experiments examining the acute effects of single-dose DPP-IV inhibitor administration on glucose tolerance may not necessarily predict the results obtained in studies with these inhibitors in different experimental paradigms. For example, DPP-IV inhibitors may exert differential effects on substrate activity in diabetic versus normoglycemic settings. Furthermore, chronic treatment with DPP-IV inhibitors has been observed to exert progressive changes in metabolic parameters beyond those detected in single-dose administration studies (51). Accordingly, analysis of the activity of DPP-IV inhibitors following prolonged administration to DIRKO mice following induction of experimental diabetes may be required to fully elucidate the complete spectrum of DPP-IV–dependent substrates contributing to improvement in glucose homeostasis.

ACKNOWLEDGMENTS

This work was supported in part by grants from the Canadian Diabetes Association (D.J.D.), the Juvenile Diabetes Research Foundation (grant nos. 1-2002-801 and 1-2000-559), and the Flemish Fund for Scientific Research (no. G.0035.03) to F.S. T.H. is supported by a Novo Nordisk-Banting and Best Diabetes Centre Studentship Award, and S.A.H. is a Visiting Postdoctoral Fellow at the FWO Vlaanderen.

The authors wish to thank Dr. C. Van Schravendijk for thoughtful discussion of the data.

REFERENCES

1. Creutzfeldt W: The incretin concept today. *Diabetologia* 16:75–85, 1979
2. Dupre J, Beck JC: Stimulation of release of insulin by an extract of intestinal mucosa. *Diabetes* 15:555–559, 1966
3. Dupre J, Ross SA, Watson D, Brown JC: Stimulation of insulin secretion by gastric inhibitory polypeptide in man. *J Clin Endocrinol Metab* 37:826–828, 1973
4. Kreymann B, Ghatei MA, Williams G, Bloom SR: Glucagon-like peptide-1 7-36: a physiological incretin in man. *Lancet* 2:1300–1304, 1987
5. Holst JJ, Orskov C, Nielsen OV, Schwartz TW: Truncated glucagon-like peptide I, an insulin-releasing hormone from the distal gut. *FEBS Lett* 211:169–174, 1987
6. Mojsov S, Weir GC, Habener JF: Insulinotropin: glucagon-like peptide I (7–37) co-encoded in the glucagon gene is a potent stimulator of insulin release in the perfused rat pancreas. *J Clin Invest* 79:616–619, 1987
7. Nauck M, Stockmann F, Ebert R, Creutzfeldt W: Reduced incretin effect in type 2 (non-insulin-dependent) diabetes. *Diabetologia* 29:46–52, 1986
8. Nauck MA, Heimesaat MM, Orskov C, Holst JJ, Ebert R, Creutzfeldt W: Preserved incretin activity of glucagon-like peptide 1 [7-36 amide] but not of synthetic human gastric inhibitory polypeptide in patients with type-2 diabetes mellitus. *J Clin Invest* 91:301–307, 1993
9. Vilsboll T, Krarup T, Deacon CF, Madsbad S, Holst JJ: Reduced postprandial concentrations of intact biologically active glucagon-like peptide 1 in type 2 diabetic patients. *Diabetes* 50:609–613, 2001
10. Tseng CC, Zhang XY, Wolfe MM: Effect of GIP and GLP-1 antagonists on insulin release in the rat. *Am J Physiol* 276:E1049–E1054, 1999
11. Baggio L, Kieffer TJ, Drucker DJ: GLP-1 but not GIP regulates fasting and non-enteral glucose clearance in mice. *Endocrinology* 141:3703–3709, 2000
12. Lewis JT, Dayanandan B, Habener JF, Kieffer TJ: Glucose-dependent insulinotropic polypeptide confers early phase insulin release to oral glucose in rats: demonstration by a receptor antagonist. *Endocrinology* 141:3710–3716, 2000
13. Miyawaki K, Yamada Y, Yano H, Niwa H, Ban N, Ihara Y, Kubota A, Fujimoto S, Kajikawa M, Kuroe A, Tsuda K, Hashimoto H, Yamashita T, Jomori T, Tashiro F, Miyazaki J, Seino Y: Glucose intolerance caused by a defect in the entero-insular axis: a study in gastric inhibitory polypeptide receptor knockout mice. *Proc Natl Acad Sci U S A* 96:14843–14847, 1999
14. Pamir N, Lynn FC, Buchan AM, Ehses J, Hinke SA, Pospisilik JA, Miyawaki K, Yamada Y, Seino Y, McIntosh CH, Pederson RA: Glucose-dependent insulinotropic polypeptide receptor null mice exhibit compensatory changes in the enteroinsular axis. *Am J Physiol Endocrinol Metab* 284:E931–E939, 2003
15. Scrocchi LA, Brown TJ, MacLusky N, Brubaker PL, Auerbach AB, Joyner AL, Drucker DJ: Glucose intolerance but normal satiety in mice with a null mutation in the glucagon-like peptide receptor gene. *Nat Med* 2:1254–1258, 1996
16. Flamez D, Van Breuseghem A, Scrocchi LA, Quartier E, Pipeleers D, Drucker DJ, Schuit F: Mouse pancreatic β-cells exhibit preserved glucose competence after disruption of the glucagon-like peptide 1 receptor gene. *Diabetes* 47:646–652, 1998
17. Pederson RA, Satkunarajah M, McIntosh CH, Scrocchi LA, Flamez D, Schuit F, Drucker DJ, Wheeler MB: Enhanced glucose-dependent insulinotropic polypeptide secretion and insulinotropic action in glucagon-like peptide 1 receptor −/− mice. *Diabetes* 47:1046–1052, 1998
18. Flamez D, Gilon P, Moens K, Van Breusegem A, Delmeire D, Scrocchi LA, Henquin JC, Drucker DJ, Schuit F: Altered cAMP and Ca^{2+} signaling in mouse pancreatic islets with GLP-1 receptor null phenotype. *Diabetes* 48:1979–1986, 1999
19. Kim JG, Baggio LL, Bridon DP, Castaigne JP, Robitaille MF, Jette L, Benquet C, Drucker DJ: Development and characterization of a glucagon-like peptide 1-albumin conjugate: the ability to activate the glucagon-like peptide 1 receptor in vivo. *Diabetes* 52:751–759, 2003
20. Krarup T, Madsbad S, Moody AJ, Regeur L, Faber OK, Holst JJ, Sestoft L: Diminished immunoreactive gastric inhibitory polypeptide response to a meal in newly diagnosed type I (insulin-dependent) diabetics. *J Clin Endocrinol Metab* 56:1306–1312, 1983
21. Deacon CF, Nauck MA, Meier J, Hucking K, Holst JJ: Degradation of endogenous and exogenous gastric inhibitory polypeptide in healthy and in type 2 diabetic subjects as revealed using a new assay for the intact peptide. *J Clin Endocrinol Metab* 85:3575–3581, 2000
22. Orskov C, Rabenhoj L, Wettergren A, Kofod H, Holst JJ: Tissue and plasma concentrations of amidated and glycine-extended glucagon-like peptide I in humans. *Diabetes* 43:535–539, 1994
23. Li Y, Hansotia T, Yusta B, Ris F, Halban PA, Drucker DJ: Glucagon-like peptide-1 receptor signaling modulates beta cell apoptosis. *J Biol Chem* 278:471–478, 2003
24. Scrocchi LA, Brown TJ, Drucker DJ: Leptin sensitivity in non-obese GLP-1 receptor−/− mice. *Diabetes* 46:2029–2034, 1997
25. Scrocchi LA, Drucker DJ: Effects of aging and a high fat diet on body weight and glucose control in GLP-1R −/− mice. *Endocrinology* 139:3127–3132, 1998
26. Orskov C, Holst JJ, Nielsen OV: Effect of truncated glucagon-like peptide-1 [proglucagon-(78-107) amide] on endocrine secretion from pig pancreas, antrum, and nonantral stomach. *Endocrinology* 123:2009–2013, 1988
27. Meier JJ, Gallwitz B, Siepmann N, Holst JJ, Deacon CF, Schmidt WE, Nauck MA: Gastric inhibitory polypeptide (GIP) dose-dependently stimulates glucagon secretion in healthy human subjects at euglycaemia. *Diabetologia* 46:798–801, 2003
28. Zawalich WS, Zawalich KC: Effects of protein kinase C inhibitors on insulin secretory responses from rodent pancreatic islets. *Mol Cell Endocrinol* 177:95–105, 2001
29. Siegel EG, Creutzfeldt W: Stimulation of insulin release in isolated rat islets by GIP in physiological concentrations and its relation to islet cyclic AMP content. *Diabetologia* 28:857–861, 1985
30. Holst JJ, Deacon CF: Inhibition of the activity of dipeptidyl-peptidase IV as a treatment for type 2 diabetes. *Diabetes* 47:1663–1670, 1998
31. Marguet D, Baggio L, Kobayashi T, Bernard AM, Pierres M, Nielsen PF, Ribel U, Watanabe T, Drucker DJ, Wagtmann N: Enhanced insulin secretion and improved glucose tolerance in mice lacking CD26. *Proc Natl Acad Sci U S A* 97:6874–6879, 2000
32. Ahren B, Simonsson E, Larsson H, Landin-Olsson M, Torgeirsson H, Jansson PA, Sandqvist M, Bavenholm P, Efendic S, Eriksson JW, Dickinson

S, Holmes D: Inhibition of dipeptidyl peptidase IV improves metabolic control over a 4-week study period in type 2 diabetes. *Diabetes Care* 25:869–875, 2002
33. Henriksen EJ, Jacob S, Fogt DL, Dietze GJ: Effect of chronic bradykinin administration on insulin action in an animal model of insulin resistance. *Am J Physiol* 275:R40–R45, 1998
34. Yang C, Chao J, Hsu WH: The effect of bradykinin on secretion of insulin, glucagon, and somatostatin from the perfused rat pancreas. *Metabolism* 46:1113–1115, 1997
35. Zhu L, Tamvakopoulos C, Xie D, Dragovic J, Shen X, Fenyk-Melody JE, Schmidt K, Bagchi A, Griffin PR, Thornberry NA, Sinha Roy R: The role of dipeptidyl peptidase IV in the cleavage of glucagon family peptides: in vivo metabolism of pituitary adenylate cyclase activating polypeptide-(1-38). *J Biol Chem* 278:22418–22423, 2003
36. Unger RH, Eisentraut AM: Entero-insular axis. *Arch Int Med* 123:261–266, 1969
37. Elrick H, Stimmler L, Hlad CJ, Arai Y: Plasma insulin responses to oral and intravenous glucose administration. *J Clin Endocrinol Metab* 24:1076–1082, 1964
38. Perley MJ, Kipnis DM: Plasma insulin responses to oral and intravenous glucose: studies in normal and diabetic subjects. *J Clin Invest* 46:1954–1962, 1967
39. Scrocchi LA, Marshall BA, Cook SM, Brubaker PL, Drucker DJ: Glucose homeostasis in mice with disruption of GLP-1 receptor signaling. *Diabetes* 47:632–639, 1998
40. Leiter EH: Mice with targeted gene disruptions or gene insertions for diabetes research: problems, pitfalls, and potential solutions. *Diabetologia* 45:296–308, 2002
41. Serre V, Dolci W, Scrocchi LA, Drucker DJ, Efrat S, Thorens B: Exendin-(9-39) as an inverse agonist of the murine GLP-1 receptor: implications for basal intracellular cAMP levels and b cell glucose competence. *Endocrinology* 139:4448–4454, 1998
42. Jamen F, Persson K, Bertrand G, Rodriguez-Henche N, Puech R, Bockaert J, Ahren B, Brabet P: PAC1 receptor-deficient mice display impaired insulinotropic response to glucose and reduced glucose tolerance. *J Clin Invest* 105:1307–1315, 2000
43. Moens K, Heimberg H, Flamez D, Huypens P, Quartier E, Ling Z, Pipeleers D, Gremlich S, Thorens B, Schuit F: Expression and functional activity of glucagon, glucagon-like peptide 1, and glucose-dependent insulinotropic peptide receptors in rat pancreatic islet cells. *Diabetes* 45:257–261, 1996
44. Huypens P, Ling Z, Pipeleers D, Schuit F: Glucagon receptors on human islet cells contribute to glucose competence of insulin release. *Diabetologia* 43:1012–1019, 2000
45. Deacon CF, Holst JJ: Dipeptidyl peptidase IV inhibition as an approach to the treatment and prevention of type 2 diabetes: a historical perspective. *Biochem Biophys Res Commun* 294:1–4, 2002
46. Drucker DJ: Therapeutic potential of dipeptidyl peptidase IV inhibitors for the treatment of type 2 diabetes. *Expert Opin Investig Drugs* 12:87–100, 2003
47. Mentlein R: Dipeptidyl-peptidase IV (CD26)–role in the inactivation of regulatory peptides. *Regul Pept* 85:9–24, 1999
48. Balkan B, Kwasnik L, Miserendino R, Holst JJ, Li X: Inhibition of dipeptidyl peptidase IV with NVP-DPP728 increases plasma GLP-1 (7-36 amide) concentrations and improves oral glucose tolerance in obese Zucker rats. *Diabetologia* 42:1324–1331, 1999
49. Deacon CF, Danielsen P, Klarskov L, Olesen M, Holst JJ: Dipeptidyl peptidase IV inhibition reduces the degradation and clearance of GIP and potentiates its insulinotropic and antihyperglycemic effects in anesthetized pigs. *Diabetes* 50:1588–1597, 2001
50. Hansotia T, Baggio L, Yamada Y, Tsukiyama S, Preitner F, Thorens B, Seino Y, Drucker DJ: Combined genetic disruption of dual incretin receptor signaling pathways reveals novel glucose lowering properties of DPP-IV inhibitors in mice (Abstract). *Diabetes* 52 (Suppl. 1):A77, 2003
51. Pospisilik JA, Stafford SG, Demuth HU, Brownsey R, Parkhouse W, Finegood DT, McIntosh CH, Pederson RA: Long-term treatment with the dipeptidyl peptidase IV inhibitor P32/98 causes sustained improvements in glucose tolerance, insulin sensitivity, hyperinsulinemia, and β-cell glucose responsiveness in VDF (fa/fa) Zucker rats. *Diabetes* 51:943–950, 2002

MOLECULAR AND CELLULAR BIOLOGY, Apr. 2004, p. 2831–2841 Vol. 24, No. 7
0270-7306/04/$08.00+0 DOI: 10.1128/MCB.24.7.2831–2841.2004

Overexpression of Inducible Cyclic AMP Early Repressor Inhibits Transactivation of Genes and Cell Proliferation in Pancreatic β Cells

Akari Inada,[1,2]† Yoshiyuki Hamamoto,[1,2] Yoshiyuki Tsuura,[1] Jun-ichi Miyazaki,[3] Shinya Toyokuni,[4] Yu Ihara,[1] Koichiro Nagai,[5] Yuichiro Yamada,[1] Susan Bonner-Weir,[2]* and Yutaka Seino[1]

Department of Diabetes and Clinical Nutrition,[1] Department of Pathology and Biology of Disease,[4] and Department of Geriatric,[5] Graduate School of Medicine, Kyoto University, Kyoto 606-8507, and Division of Stem Cell Regulation Research G6, Medical School, Osaka University, Suita, Osaka 565-0871,[3] Japan, and Section of Islet Transplantation and Cell Biology, Joslin Diabetes Center, Harvard Medical School, Boston, Massachusetts 02215[2]

Received 29 September 2003/Returned for modification 18 December 2003/Accepted 5 January 2004

Transcriptional control mediated by the cyclic AMP-responsive element (CRE) represents an important mechanism of gene regulation. To test our hypothesis that increased inducible cyclic AMP early repressor (ICER) Iγ inhibits function of CRE-binding proteins and thus disrupts CRE-mediated transcription in pancreatic β cells, we generated transgenic mice with β-cell-directed expression of ICER Iγ, a powerful repressor that is greatly increased in diabetes. Three transgenic lines clearly show that increased ICER Iγ expression in β cells results in early severe diabetes. From birth islets were severely disorganized with a significantly increased proportion of α cells throughout the islet. Diabetes results from the combined effects of impaired insulin expression and a decreased number of β cells. The decrease in β cells appears to result from impaired proliferation rather than from increased apoptosis after birth. Cyclin A gene expression is impaired by the strong inhibition of ICER; the suppression of cyclin A results in a substantially decreased proliferation of β cells in the postnatal period. These results suggest that CRE and CRE-binding factors have an important role in pancreatic β-cell physiology not only directly by regulation of gene *trans*-activation but also indirectly by regulation of β-cell mass.

Transcriptional control of pancreatic hormone genes is mediated by specific combinations of positive- and negative-acting factors (4, 10–12, 16, 40, 51, 54) through multiple *cis*-acting elements that are influenced by changes in glucose or cyclic AMP levels (19, 42, 45, 46, 55). One of the elements, the cyclic AMP-responsive element (CRE), has been shown to be an important determinant of gene expression in pancreatic islet cells (6, 13, 18, 30, 34, 43, 44, 47). While the function of its transcriptional activators has been studied extensively, much less is known about the actions and the physiological importance of transcriptional repressors.

CRE modulator (CREM) is a unique gene that generates by alternative splicing both transcriptional activators and repressors (14). These products show cell-, tissue-, and development-specific patterns of expression and play key physiological and developmental roles in regulating gene transcription through CREs (7). One of the isoforms, inducible cyclic AMP early repressor (ICER), is transcribed from an intronic promoter of the CREM gene and consists of only a DNA-binding domain (DBD) (41). The activity of ICER is greatly influenced by its intracellular concentration, because once increased it down-regulates its own expression, establishing an autoregulatory feedback loop (15). The induction of this powerful repressor is important for the transient nature of cyclic AMP-induced gene expression (8). ICER has been shown to be dramatically up-regulated by treatment with forskolin (39) but not by Ca^{2+} (35). Recently, it was reported that ICER expression in pancreatic β cells was powerfully induced by glucagon (27) and increased in diabetes (28). The binding activity of ICER is more efficient than that of CREM activator, enabling it to competitively block the binding of the CREM activator or other members of the CREB/ATF family (29), such as CREB, ΔCREB, and CRE-BP1 (17, 21, 31, 38).

Here we further examined the roles of CRE and CRE-binding activator in the pancreatic β cell by cell-specific overexpression of repressor ICER Iγ in transgenic (Tg) mice. Overexpressed ICER Iγ can compete with endogenous CRE-binding activators to block CRE-mediated transcription and result in diabetes.

MATERIALS AND METHODS

Generation of ICER Iγ Tg mice. The pCMV-ICER Iγ expression plasmid carrying the cDNA for rat ICER Iγ has been described previously (29). ICER Iγ cDNA (encoding amino acids 1 to 108 [TAA]) was excised from pCMV-ICER Iγ as an EcoRI/EcoRI fragment and was inserted into exon 3 of rabbit β-globin downstream of the human insulin promoter in the Tg plasmid pIns-1 (25). The transgene cassettes (Fig. 2A) were excised from the resulting pIns-ICER Iγ plasmid by restriction enzyme digestion to exclude plasmid-derived sequences, and linearized cassettes were microinjected into fertilized eggs of C57BL/6 × C57BL/6 mice (Japan SLC Inc., Nagoya, Japan). Tg mice were identified by PCR

* Corresponding author. Mailing address: Section of Islet Transplantation and Cell Biology, Joslin Diabetes Center, Harvard Medical School, One Joslin Place, Boston, MA 02215. Phone: (617) 732-2581. Fax: (617) 732-2650. E-mail: susan.bonner-weir@joslin.harvard.edu.

† Present address: Section of Islet Transplantation and Cell Biology, Joslin Diabetes Center, Harvard Medical School, Boston, MA 02215.

analysis of tail DNA. The transgene copy number in founder mice was estimated from Southern blot signal intensity compared to indicator bands of the endogenous gene by using NIH Image. Signal intensity was obtained as PICT files by a slide scanner (Polascan 35; Polaroid, Tokyo, Japan), and the PICT file was opened in gray-scale mode by NIH Image. In all experiments, non-Tg littermates (wild type [WT]) were used for controls. All mice were handled in accordance with the guidelines for animal experiments of Kyoto University. The data presented here are from males only (line Tg23 except where noted), but similar results were obtained in females.

DNA analysis. Southern blot assays were performed with genomic DNA digested with EcoRI. A probe in exons γ, H, and Ia of the ICER gene was hybridized to a fragment specific for the transgene. Genotyping by PCR was performed with genomic DNA and oligonucleotide primers *e* and *f* (Fig. 2A), designed to hybridize to rabbit β-globin and exon H of the ICER gene. The transgene-specific products were amplified with 40 cycles of PCR and visualized with ethidium bromide in 1.5% agarose gels.

Measurements of blood glucose levels and serum parameters. Blood glucose levels were determined by an enzyme-electrode method with Glutest (Sanwa Kagaku Kenkyusho, Nagoya, Japan) on whole blood taken from the tail vein. For other parameters, blood was withdrawn from the heart immediately before isolation of the pancreatic islets under pentobarbital anesthesia. Serum parameters were determined using the following enzyme-linked immunosorbent assay kits: insulin (Morinaga Institute of Biological Science, Yokohama, Japan), ketones (Sanwa Kagaku Kenkyusho), and glucagon (Yanaihara Institute Inc., Shizuoka, Japan).

Oral glucose tolerance test (OGTT) and insulin release test. After a 16-h fast 10-week-old male mice (n = 10 in each group) were loaded with glucose (1 g kg of body weight^{-1}) by gavage. Blood samples were collected from the tail vein at 0, 15, 30, 60, 90, and 120 min for glucose; serum insulin concentrations were determined for samples at 0, 15, and 30 min.

Isolation of pancreatic islets, insulin secretion, and content. Pancreatic islets from Tg (n = 5) and WT (n = 5) mice at 12 weeks of age were isolated by collagenase digestion, followed by purification on Ficoll gradients. Insulin secretion, insulin content, and DNA content of freshly isolated islets matched for size were assessed using the batch incubation method, radioimmunoassay, and fluorometric assays, respectively, as described previously (23). Three independent isolations and/or experiments were performed.

RNA isolation, reverse transcription-PCR, and Northern blotting. Total RNA was extracted from freshly isolated islets of Tg (n = 10) and WT (n = 10) mice at 10 weeks of age with Trizol reagent (GIBCO) according to the manufacturer's instructions and used as a template for cDNA synthesis (Superscript reverse transcriptase [Life Technologies]) and for Northern blotting. Mouse pancreatic islet cDNA was amplified by PCR with rabbit β-globin and ICER-specific oligonucleotides. To exclude any amplification product derived from genomic DNA that could contaminate the RNA preparation, total RNA without reverse transcription was amplified as a negative control. To determine the expression of the transgene, the primers *d* and *f* (Fig. 2A) were designed to span an intron of the rabbit β-globin gene to distinguish transgene mRNA and genomic DNA. Since the transgene construct carried a rabbit β-globin intron-splice signal, correct expression of the transgene could be identified by a smaller PCR product lacking the inserted β-globin intron sequence compared with the PCR from genomic DNA. Northern blotting was performed with a rat insulin cDNA probe with total islet RNA (20 μg). Probe labeling and detection were performed according to the protocol given in the Gene Images random prime labeling and detection system (Amersham Pharmacia Biotech).

Semiquantitative PCR. The mRNA expression in islets of WT and Tg mice was quantified by semiquantitative PCR as described previously (28). Isoform-specific primers *a* to *c* were set to determine the expression of CREM and ICER Iγ (Fig. 1A). The number of amplification cycles was selected such that the amplification of each sequence was in the exponential phase of the amplification curve. For ICER Iγ, CREM activator, TATA-binding protein, and cyclin A mRNA, the exponential portion of the curve corresponds to 37 cycles. The amount of [α-^{32}P]dCTP incorporated into each amplimer was measured on a PhosphorImager and quantified with ImageQuant software (Molecular Dynamics, Sunnyvale, Calif.). TATA-binding protein was used to control for differences in overall cDNA concentration and experimental variations between samples. The amount of each specific product was expressed relative to this internal control, giving a specific product/control gene ratio for each sample.

Cell culture and transfection. Cell culture and transient transfection in HIT-T15 cells (hamster pancreatic β-cell line) were performed as described previously (29). The cells were transfected using Lipofectamine (GIBCO) with a mixture of the luciferase reporter plasmid, containing the human insulin gene promoter or the rat cyclin A gene promoter (kindly provided by K. Oda and A. Takeuchi, Science University of Tokyo, Chiba, Japan [53]), CREMτα or ICER Iγ expression plasmid (29), and internal control p-act-β-gal. Forty-eight hours after transfection, the cells were harvested and cell extracts were prepared for luciferase assays and β-galactosidase assays. β-Galactosidase assays were performed for internal control. Luciferase activity was normalized to the background activity obtained from the transfection of the promoterless luciferase plasmid in the same experiments. Transfection experiments were repeated more than three times. The data presented here are from rat cyclin A only, but similar results were obtained using mouse cyclin A promoter (kindly provided by M. Schorpp-Kistner, Deutsches Krebsforschungszentrum Heidelberg, Heidelberg, Germany [2]).

Immunohistochemistry. WT (n = 5 for each age except 7 days, for which n = 7) and Tg (n = 5 for each age except 7 days, for which n = 9) mouse pancreases were fixed in 10% buffered formalin, embedded in paraffin, and cut in serial (5-μm) sections. The following primary antibodies were used: anti-ICER (antiserum α-CREM S4; 1:500; kindly provided by J. F. Habener, Massachusetts General Hospital, Howard Hughes Medical Institute, Boston, Mass. [5, 27]), anti-insulin (1:500; DAKO); antiglucagon (1:350; OAL-123; Otsuka Assay Laboratory, Tokushima, Japan, or Linco); anti-islet amyloid polypeptide (IAPP; 1:50; gift of C. B. Verchere, VA Medical Center, Seattle, Wash.), anti-cyclin A (1:50; Santa Cruz Biotechnology), and anti-Ki67 (1:200; PharMingen). Primary antibody was detected by immunofluorescence labeling with fluorescein isothiocyanate-conjugated or Texas red-conjugated secondary antibodies or by immunoperoxidase with biotin-labeled secondary antibodies. Staining was visualized with alkaline phosphatase substrate (Vector Laboratories, Burlingame, Calif.) or diaminobenzidine. For proliferation studies, pancreatic sections of 7-day-old mice were double immunostained for insulin and Ki67; all (insulin-positive) islets per single section per animal were photographed using a Zeiss LSM 410 confocal microscope. Images of all insulin-positive cells were evaluated for expression of the cell cycle marker Ki67. For apoptosis studies, terminal deoxynucleotidyltransferase-mediated dUTP-biotin nick end labeling (TUNEL) staining was performed according to the manufacturer's instructions (in situ cell death detection POD kit; Roche) on pancreatic sections of 7-day-old mice (n = 4 for each group).

RESULTS

Blocking CRE-mediated transcription by ICER Iγ. A schematic representation of the structure of the CREM isoforms is shown in Fig. 1A. The CREM gene consists of 10 exons, A to I, including functional domains, two glutamine-rich domains (Q1 and Q2), the phosphorylation domain (P box), and the DBD. CREMτα is a full-length isoform and contains activation domains, thus functioning as an activator (14), but ICER Iγ is transcribed from an alternative intronic promoter (P2) and consists only of DBD. A remarkable reduction in insulin and cyclin A gene transcription was observed when CREs were mutated in both humans (9, 30) and rodents (2, 44, 53), so transcription factors that bind to the CRE might play an important role in the regulation of these two genes. To test the effect of CREM and ICER Iγ on insulin and cyclin A gene transcription, HIT-T15 cells were transfected with a luciferase reporter plasmid containing the human insulin promoter or the rat cyclin A promoter (Fig. 1B and C). The insulin-luciferase reporter contains four functional CREs. CREMτα produced high levels of luciferase activity, while ICER Iγ repressed activity. When cotransfected, ICER Iγ substantially repressed CREMτα-induced activity (Fig. 1B). The rat cyclin A-luciferase reporter gene contained one CRE, and again, ICER Iγ repressed promoter activity (Fig. 1C). In the presence of mutated CRE, no effect of ICER Iγ was observed, suggesting that ICER Iγ competes and blocks the activities of transcriptional activators through CRE (Fig. 1D).

Production of ICER Iγ Tg mice. To test our hypothesis that increased ICER Iγ blocks CRE-mediated transcription in vivo, we generated Tg mice expressing ICER Iγ in pancreatic β cells

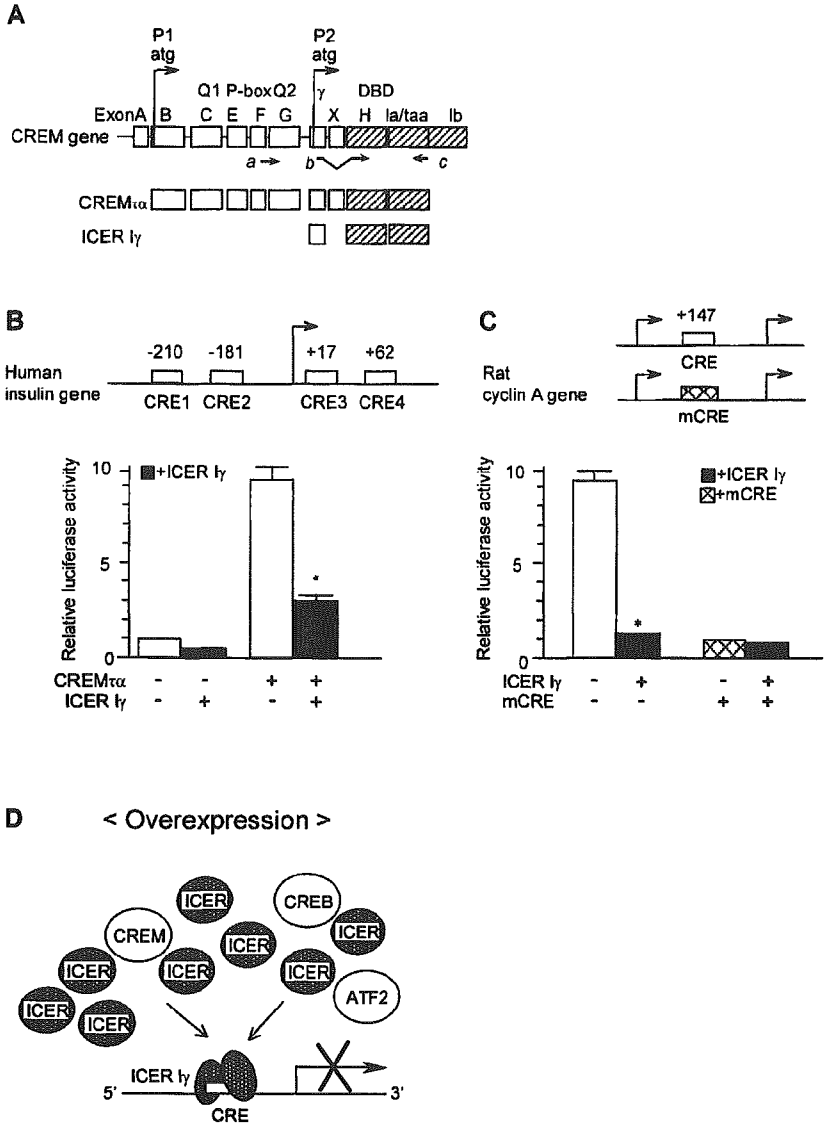

FIG. 1. (A) Schematic presentation of the structure of the CREM gene and isoforms. CREMτα contains activation domains (Q1, Q2, P box, and the DBD) and functions as an activator. ICER Iγ is transcribed from an alternative intronic promoter (P2) and contains only the DBD. The arrows, *a* to *c*, represent the positions of synthetic oligonucleotide primers used to detect specific isoforms. (B and C) Transient-expression studies analyzing the effect of ICER Iγ in CRE-mediated transcription. ICER Iγ or CREMτα expression plasmids were transfected into HIT-T15 cells (pancreatic β-cell line) with the luciferase reporter plasmid containing the human insulin gene promoter (B) or the rat cyclin A promoter gene (C). To determine if ICER Iγ represses not only basal promoter activity but also CREMτα-induced promoter activity, the same amount of ICER Iγ expression plasmid was cotransfected with the expression plasmid of CREMτα. Solid bars represent cotransfection with ICER Iγ. These transfections were repeated more than three times. *, $P < 0.05$. (D) The hypothesis of this study is that increased ICER Iγ can compete with other members of the CREB/ATF family and disrupt CRE-mediated transcription.

(Fig. 2A). Three mice carrying the transgene were identified among 62 potential founders. These mice were used to establish three ICER Iγ Tg lines, designated Tg7, Tg12, and Tg23 (Table 1). Reverse transcription-PCR with primers *d* and *f* to detect transgene expression showed a shorter PCR product (Fig. 2B, lane 2) for the transgene than for the genomic DNA template (lane 1) due to the excision of the rabbit β-globin intron sequence. To compare the mRNA levels of ICER Iγ and CREM activator in Tg and WT mouse islets, semiquantitative PCR was carried out using primers *a* to *c* (Fig. 1A). The expression level of ICER Iγ in islets of Tg mice was increased (Fig. 2C), but there was no significant difference in the expression of CREM activator between Tg and WT mice. To determine ICER protein expression, pancreatic sections of 7-day-old mice were double stained with anti-insulin and anti-ICER antibodies. ICER protein (red) was present only in nuclei of β cells (green) in islets and single insulin-positive cells in Tg mouse pancreas but was at an undetectable level in WT mouse pancreas (Fig. 2D).

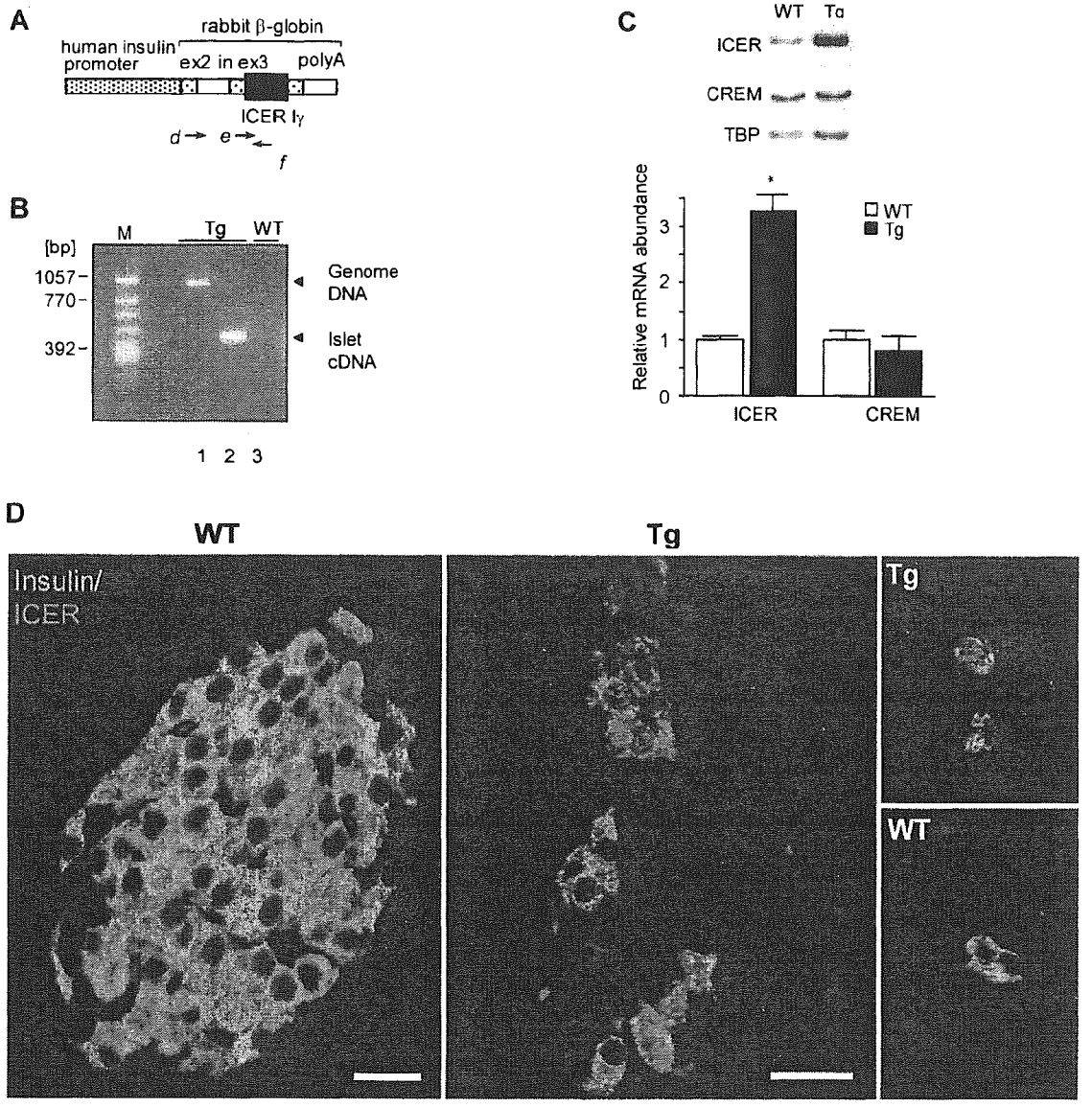

FIG. 2. Generating ICER Iγ Tg mice. (A) The transgene contains the human insulin promoter, an intron (in), a part of exons 2 and 3 (ex2 and ex3), a poly(A) signal from the rabbit β-globin gene, and ICER Iγ cDNA. The transcribed mRNA contains ex2, ex3, and ICER Iγ but is translated into only the ICER Iγ protein. (B) Analysis of expression of the transgene in pancreatic islets was performed using primers *d* and *f*. Shorter PCR products show correct expression of the transgene in which the intron was spliced into Tg mouse islet cDNA ($n = 10$) (lane 2). Tg mouse genomic DNA with an intron and WT mouse islet cDNA without any transgene fragments were used as controls (lanes 1 and 3, respectively) (line Tg23). (C) The ICER Iγ and CREM activator mRNA levels in islet cells were determined by semiquantitative PCR (line Tg23). After normalization to the control gene, the mRNA levels are expressed relative to the level of WT mRNA. TBP, TATA-binding protein. *, $P < 0.05$. (D) For determination of ICER protein expression in β cells, dual staining of pancreatic sections at day 7 with anti-insulin and anti-ICER antibody was analyzed by confocal microscopy (line Tg23). ICER protein (red) was present in nuclei of insulin-positive β cells (green) in Tg but not WT mice. Bars, 10 μm.

ICER Iγ transgene expression results in severe diabetes. ICER Iγ Tg mice develop severe diabetes early in life. Blood glucose levels are normal at birth (day 0) (80 ± 21 mg/dl) but moderately elevated at day 7 (209 ± 21 mg/dl) (Fig. 3A) and further elevated by 2 weeks of age; blood glucose levels remained high until death at 20 to 36 weeks (Fig. 3B). Plasma insulin concentrations were extremely low, being only 20% of WT level at 6 weeks (WT versus Tg mice, 1,282 ± 87 versus 288 ± 45 pg/ml, respectively; $P < 0.001$) (Fig. 3C). Blood ketone levels were markedly elevated at 6 and 12 weeks of age and increased further before death (Fig. 3D). The plasma glucagon levels were also quite high (Fig. 3E). Upon oral glucose challenge (OGTT), blood glucose levels were substantially increased at 15 min and gradually declined to basal levels by 120 min in WT mice but remained abnormally high throughout the 120-min period in Tg mice (Fig. 3F, left). Glucose

TABLE 1. Comparison of serum parameters and body weights at 12 weeks of age among ICER Iγ Tg mouse lines[c]

Mouse line	Copy no.	Body wt (g)		Body glucose concn (mg/dl)		Plasma insulin concn (pg/ml)	
		M	F	M	F	M	F
Control	0	33.2 ± 0.9	21.7 ± 0.7	153 ± 4.1	126 ± 9.9	1,350.3 ± 194.5	1,480.7 ± 19.4
Tg7	4	25.8 ± 1.7[a]	21.8 ± 0.6	527 ± 52.8[a]	355 ± 61.7[b]	350.3 ± 80.0[a]	422.4 ± 130[a]
Tg12	4	22.7 ± 2.6[a]	22.5 ± 0.9	528 ± 62.1[a]	336 ± 93.2[b]	545.6 ± 183.7[b]	654.6 ± 84.2[b]
Tg23	6	21.7 ± 2.4[a]	22.6 ± 1.0	551 ± 31.1[a]	420 ± 59.5[b]	278.1 ± 111.2[a]	445.5 ± 39.7[a]

[a] $P < 0.05$ versus control.
[b] $P < 0.001$ versus control.
[c] Three mice positive for the transgene were founders of three ICER Iγ Tg lines, Tg7, Tg12, and Tg23. Results are means ± standard errors of at least 10 animals from each line. M, male; F, female.

levels were about twice as high in Tg as in WT mice at all time points. The plasma insulin response following OGTT was also markedly impaired in Tg mice, being reduced by 70 to 80% at all time points (Fig. 3F, right).

We compared serum parameters and body weights in males and females of the three Tg lines (Table 1) at 12 weeks of age. Although lines Tg7 and Tg12 had four copies of the transgene and line Tg23 had six copies, there were no significant differences in weight or blood glucose or plasma insulin levels among the three Tg lines. All were hyperglycemic with decreased plasma insulin levels, suggesting that the amount of ICER in each line was effective. This in vivo finding is consistent with the in vitro effect of ICER expression on insulin promoter activity in HIT-T15 cells (29). Body weight was markedly reduced in the male Tg mice at 12 weeks of age, but in the female mice only by 20 weeks of age. In a longitudinal study of Tg23 male mice, body weight was similar to that of controls until 4 weeks of age, at which point Tg mice failed to gain weight, with only slight growth after 8 weeks of age (Fig. 4).

Together, these results show that overexpression of ICER Iγ in pancreatic β cells is associated with early severe diabetes.

Isolated islets from ICER Iγ Tg mice. In static incubations isolated WT mouse islets had dose-dependent glucose-induced insulin secretion, but Tg mouse islets had greatly reduced insulin secretion (Fig. 5A). In comparison to isolated islets matched for size, Tg mouse islets were only 18% reduced in DNA level but 95% reduced in insulin content (WT versus Tg mice, 65.2 ± 3.7 versus 2.8 ± 0.55 ng of insulin/islet, respectively) (Fig. 5B). In islets isolated from 10-week-old mice, insulin mRNA expression was significantly reduced in Tg mice, with a weak band observed only in female Tg mice (Fig. 5C). Ultrastructural analysis showed a markedly reduced number of insulin secretory granules within individual β cells of Tg mice (Fig. 5D) compared to WT mice.

ICER Iγ Tg mice exhibit abnormal islet morphology. To assess islet morphology, pancreatic sections from 0-day-old (nondiabetic condition) to 36-week-old (severe diabetes) mice were immunostained for insulin and glucagon. In controls, the typical islet morphology of a core of insulin-positive cells with a mantle of glucagon-positive cells was seen (Fig. 6A). In Tg mice, however, even at day 0, there were far fewer insulin-positive cells, so the islets appeared severely disorganized with an increased proportion of glucagon-positive cells; this pattern did not differ with age. At 7 days of age, when animals were becoming hyperglycemic, differential expression of insulin by immunostaining was observed within the same islet (Fig. 6B), with some cells having clear staining and others having almost none. To demonstrate the presence of degranulated β cells, IAPP was used as a β-cell marker (Fig. 6C). Again, β cells were reduced in number and most of the islet was glucagon positive. A few cells coexpressing IAPP and glucagon were present in Tg mice. These morphological abnormalities were already apparent at day 0 and in the late fetal period (data not shown), indicating that these changes are a direct result of the increased ICER Iγ and not due to hyperglycemia.

ICER Iγ Tg mice exhibit reduced β-cell proliferation. Since β-cell mass is regulated by a balance of cell renewal (neogenesis from precursors and proliferation of β cells) and cell loss through apoptosis, these determinants of β-cell mass were examined. While it is difficult to assess neogenesis, scattered singlets-doublets of insulin-positive cells were as frequent in Tg as WT mice at 7 days of age (Fig. 6D), suggesting that neogenesis of β cells was not impaired. Using TUNEL staining, no morphological evidence of increased apoptosis at 7 days of age was seen (data not shown). To evaluate β-cell proliferation, dual staining of Ki67 and insulin was performed on 7-day-old mouse pancreases. Ki67 protein was detected in many nuclei of insulin-positive cells in WT mice but in no insulin-positive cells in Tg mice (WT mice, 12 islets, 160 Ki67-positive, insulin-positive cells of 512 insulin-positive cells; Tg mice, 5 islets, 0 Ki67-positive, insulin-positive cells of 103 insulin-positive cells) (Fig. 7A). Since both CREM and ICER have been reported to regulate the cell cycle by modulating cyclin A gene expression (43) (Fig. 1C), cyclin A expression was measured. At day 7, normally a time of active islet proliferation, cyclin A protein, as detected by immunostaining, was seen in most nuclei in WT mouse islets but in only a few cells of Tg mouse islets (Fig. 7B) even though there was no difference in cyclin A immunostaining in acinar cells between Tg and WT mice. In agreement with this, cyclin A mRNA levels, determined by semiquantitative PCR, were decreased in Tg mouse islets (Fig. 7C). These data suggest that ICER Iγ represses cyclin A gene transcription in β cells, which in turn may limit β-cell proliferation. The neonatal period is one of enhanced replication and neogenesis and active apoptosis in normal rodent pancreas, but in these ICER Tg mice the decreased number of β cells is likely to be due to the decreased proliferation rather than increased apoptosis.

DISCUSSION

First, we demonstrated that CREMτα functions as an activator of insulin and cyclin A promoters, whereas ICER Iγ acts as a strong repressor. Previously, we have reported that the

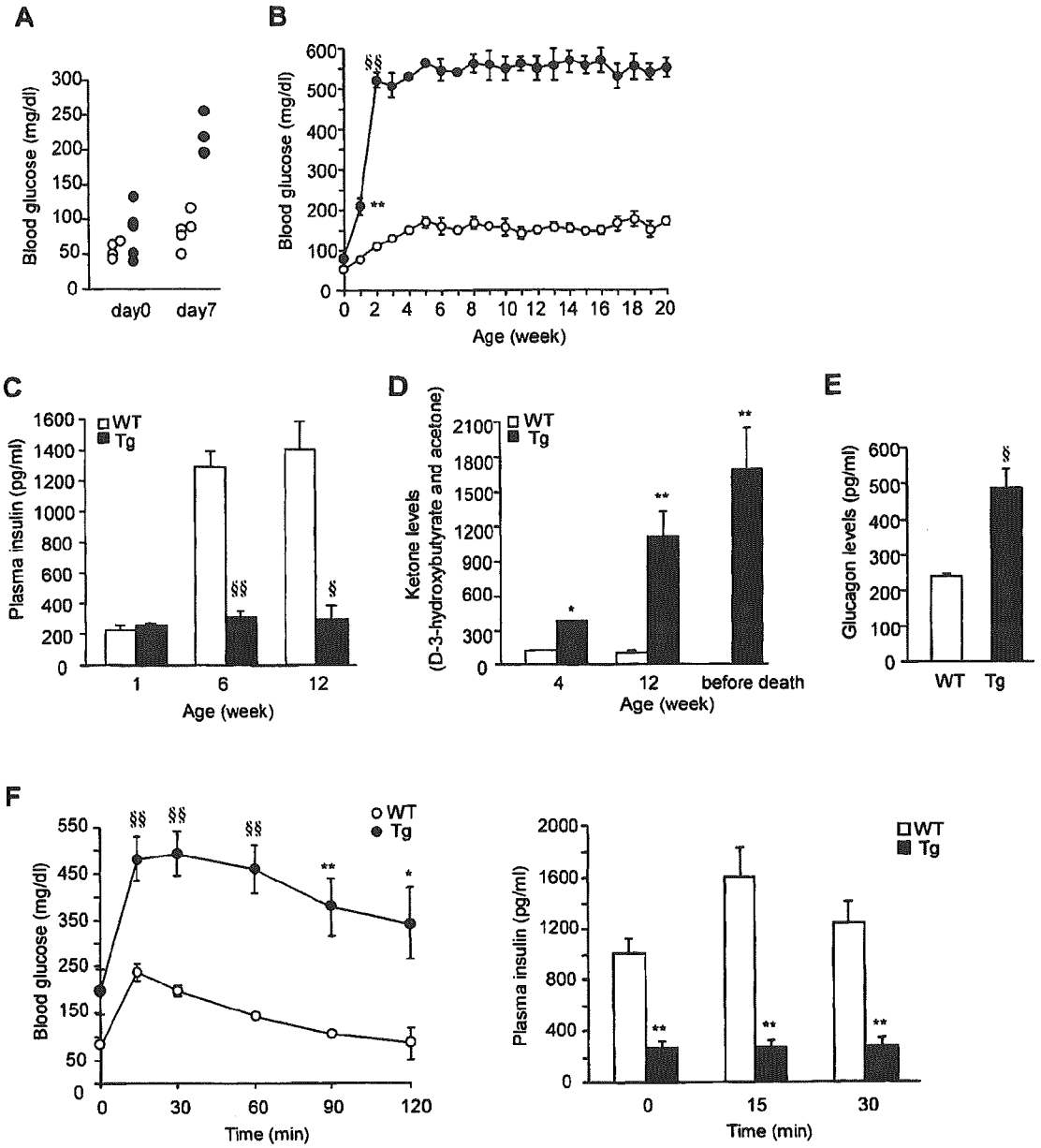

FIG. 3. Severe diabetes in ICER Iγ Tg mice. (A and B) Blood glucose levels; (C) fed plasma insulin levels; (D) blood ketone levels; (E) plasma glucagon levels (line Tg23); (F) OGTT and insulin release in ICER Iγ Tg mice at 10 weeks of age (line Tg12). Tg (n = 10) and WT (n = 10) mice were fasted for 16 h before the study and then were given glucose (1 g kg of body weight^{-1}). Left, plasma blood glucose levels at indicated times; right, plasma insulin levels at 0, 15, and 30 min after oral glucose load. Solid and open bars or circles represent Tg and WT mice, respectively. *, $P < 0.05$; **, $P < 0.01$; §, $P < 0.005$; §§, $P < 0.001$.

efficiency of binding of ICER Iγ to CRE was higher than that of CREMτα and so it competitively inhibited the binding of CREMτα (29). Those in vitro results suggested that increased ICER Iγ in pancreatic β cells could compete with endogenous members of the CREB/ATF family such as CREM (7), CREB (18), CRE-BP1 (31, 38), and ATF (21) and disrupt CRE-mediated insulin and cyclin A gene transcription in vivo. To test our hypothesis, we directly assessed in vivo the effects of increasing ICER Iγ in pancreatic β cells.

Since it is important to determine the specificity for the effect of ICER Iγ overexpression in pancreatic β cells, we established three Tg lines. Although the three lines contained different copy numbers of the transgene, all had normal blood glucose levels at birth, but within days their blood glucose levels increased dramatically and the mice developed severe diabetes characterized by polydipsia, polyuria, reduced serum insulin levels, and elevated ketone and glucagon levels. There was a profound depletion of insulin cells already during the late fetal period, preceding any hyperglycemia, which was evident only by 7 days of age. Insulin secretion from islets was